SUPPLEMENTAL INFORMATION

Suppression and Synthetic-Lethal Genetic Relationships of Δ*gpsB* Mutations Indicate That GpsB Mediates Protein Phosphorylation and Penicillin-Binding Protein Interactions in *Streptococcus pneumoniae* D39

Britta E. Rued[1§], Jiaqi J. Zheng[1§], Andrea Mura[2], Ho-Ching T. Tsui[1], Michael J. Boersma[1], Jeffrey L. Mazny[1], Federico Corona[2], Amilcar J. Perez[1], Daniela Fadda[2], Linda Doubravová[3], Karolína Buriánková[3], Pavel Branny[3], Orietta Massidda[2], and Malcolm E. Winkler[1]*

[1]Department of Biology, Indiana University Bloomington, Bloomington, IN 4705, USA

[2]Dipartimento di Scienze Chirurgiche, Università di Cagliari, 09100 Cagliari, Italy

[3]Cell and Molecular Microbiology Division, Institute of Microbiology, v.v.i., Academy of Sciences of the Czech Republic, 142 20 Prague 4, Czech Republic

Running title: Functions of essential pneumococcal GpsB in division

[§]Contributed equally to this work.

*Corresponding author E-mail: winklerm@indiana.edu

Tables S1-S8

Figures Legends for Supplemental Figures S1-S15

References for Supplemental Information

TABLE S1. *Streptococcus pneumoniae* strains used in this study[a]

***S. pneumoniae* strains**			
Strain Number	Genotype (description)[b]	Antibiotic resistance[c]	Reference or source
E46	D39 Δ*cps* Δ*bgaA*::P_c-*erm* (IU1945 transformed with fusion Δ*bgaA*::P_c-*erm* amplicon)	Erm^R	This study
E177	D39 Δ*cps* ∆*pbp1a*::P_c-e*rm*	Erm^R	(Land *et al.*, 2013)
E180	D39 Δ*cps* ∆*pbp2a*::P_c-e*rm*	Erm^R	(Land *et al.*, 2013)
E193	D39 Δ*cps* ∆*pbp1b*::P_c-e*rm*	Erm^R	(Land *et al.*, 2013)
E736	D39 Δ*cps* Δ*phpP*::P_c-*erm* (IU1945 transformed with fusion Δ*phpP*::P_c-*erm* amplicon)	Erm^R	This study
E739	D39 Δ*cps* Δ[*phpP-stkP*]::P_c-*erm* (IU1945 transformed with fusion Δ[*phpP-stkP*]::P_c-*erm* amplicon)	Erm^R	This study
EL59	R6	None	(Hoskins *et al.*, 2001)
IU1690	D39	None	(Lanie *et al.*, 2007)
IU1781	D39 *rpsL1*	Str^R	(Ramos-Montanez *et al.*, 2008)
IU1824	D39 *rpsL1* ∆*cps2A'-cps2H'* = D39 *rpsL1* ∆*cps*	Str^R	(Lanie *et al.*, 2007)
IU1945	D39 Δ*cps*	None	(Lanie *et al.*, 2007)
IU3297	D39 Δ*cps rpsL1* Δ*divIVA*::P_c-[*kan-rpsL*$^+$] (IU1781 transformed with fusion amplicon Δ*divIVA*::P_c-[*kan-rpsL*$^+$])	Kan^R	This study
IU4846	D39 Δ*cps* Δ*bgaA::kan-t1t2-*P_{fcsk}*-gpsB*	Kan^R	(Land *et al.*, 2013)
IU4888	D39 Δ*cps* Δ*gpsB*<>*aad9*//Δ*bgaA::kan-t1t2-*P_{fcsk}*-gpsB*	Kan^R Spc^R	(Land *et al.*, 2013)
IU5456	D39 Δ*cps ezrA*-L-$FLAG^3$-P_c-*erm* (IU1945 transformed with fusion amplicon, *ezrA*-L-$FLAG^3$-P_c-*erm*)	Erm^R	This study
IU5458	D39 ∆*cps gpsB*-L-$FLAG^3$-P_c-*erm*	Erm^R	(Land *et al.*, 2013)
IU5838	D39 ∆*cps gpsB*-FLAG-P_c-*erm*	Erm^R	(Land *et al.*, 2013)
IU5845	D39 Δ*cps* Δ*gpsB*<>*aad9* Δ[*spd1026-spd1037*] Ω[*spd_0889-spd_1026*] (IU1945 transformed with Δ*gpsB*<>*aad9* amplicon from IU4888, with other mutations arising spontaneously) Sup2 in Figure 3.	Spc^R	This study
IU6441	D39 Δ*cps* Δ*gpsB*<>*aad9* Δ[*spd1029-spd1037*] Ω[*spd_0889-spd_1024*] (IU1945 transformed with Δ*gpsB*<>*aad9* amplicon from IU4888,	Spc^R	This study

	with other mutations arising spontaneously) Sup3 in Figure 3.		
IU6442	D39 Δ*cps* Δ*gpsB*<>*aad9 phpP*(G229D) (IU1945 transformed with Δ*gpsB*<>*aad9* amplicon from IU4888, with spontaneous *phpP*(G229D) mutation) Sup1 in Figure 3.	Spc^R	This study
IU6444	D39 Δ*gpsB*<>*aad9 phpP*(G117D) (IU1945 transformed with Δ*gpsB*<>*aad9* amplicon from IU4888, with spontaneous *phpP*(G117D) mutation)	Spc^R	This study
IU6543	D39 Δ*cps pbp2b*-FLAG-P_c-*erm*	Erm^R	(Tsui *et al.*, 2014)
IU6741	D39 Δ*cps rpsL1* Δ*pbp1a*	Str^R	(Tsui *et al.*, 2016)
IU6810	D39 Δ*cps ezrA*-HA-P_c-*kan* (IU1945 transformed with fusion amplicon *ezrA*-HA-P_c-*kan*)	Kan^R	This study
IU6929	D39 Δ*cps pbp2x*-HA-P_c-*kan*	Kan^R	(Land *et al.*, 2013)
IU6933	D39 Δ*cps pbp2b*-HA-P_c-*kan*	Kan^R	(Tsui *et al.*, 2014)
IU6962	D39 *Δcps ftsZ*-Myc-P_c-*kan*	Kan^R	(Land *et al.*, 2013)
IU7242	D39 Δ*cps pbp1a*-HA-P_c-*kan* (IU1945 transformed with fusion *pbp1a*-HA-P_c-*kan* amplicon)	Kan^R	This study
IU7426	D39 Δ*cps pbp2b*-HA^4-P_c-*kan*	Kan^R	(Tsui *et al.*, 2014)
IU7434	D39 Δ*cps stkP*-$FLAG^2$-P_c-*erm*	Erm^R	(Tsui *et al.*, 2014)
IU7438	D39 Δ*cps stkP*-HA-P_c-*kan*	Kan^R	(Tsui *et al.*, 2014)
IU7510	D39 Δ*cps pbp2x*-HA-P_c-*kan stkP*-$FLAG^2$-P_c-*erm*	Kan^R Erm^R	(Tsui *et al.*, 2014)
IU7512	D39 Δ*cps pbp2b*-HA-P_c-*kan stkP*-$FLAG^2$-P_c-*erm*	Kan^R Erm^R	(Tsui *et al.*, 2014)
IU7614	D39 Δ*cps rpsL1 ftsZ*-P_c-[*kan-rpsL*$^+$] (IU1824 transformed with fusion amplicon, *ftsZ*-P_c-[*kan-rpsL*$^+$])	Kan^R	(Tsui *et al.*, 2016)
IU7644	D39 Δ*cps pbp2b*-HA^4-P_c-*erm* (IU1945 transformed with *pbp2b*-HA^4-P_c-*erm* fusion amplicon)	Erm^R	This study
IU7649	D39 Δ*cps phpP*$^+$-P_c-[*kan-rpsL*$^+$] (IU1945 was transformed with fusion amplicon *phpP*$^+$-P_c-[*kan-rpsL*$^+$])	Kan^R	This study
IU7667	D39 Δ*cps rpsL1 ftsZ*-Myc (IU7614 transformed with fusion amplicon, *ftsZ*-Myc)	Str^R	This study
IU7673	D39 Δ*cps rpsL1 phpP*$^+$-P_c-[*kan-rpsL*+]-*stkP*$^+$ (IU1824 was transformed with *phpP*$^+$-P_c-[*kan-rpsL*$^+$] from IU7649)	Kan^R	This study
IU7685	D39 Δ*cps rpsL1 phpP*(G229D) *stkP*(G10stop) (IU7673 was transformed with *phpP*(G229D) amplicon from IU6442 with spontaneous *stkP*(G10 stop) mutation)	Str^R	This study

IU7733	D39 Δ*cps rpsL1* Δ*gpsB<>aad9 phpP*(G229D) *stkP*(G10 stop) (IU7685 was transformed with Δ*gpsB<>aad9* from IU4888)	Spc^R, Str^R	This study
IU7736	D39 Δ*cps rpsL1* Δ*gpsB<>aad9 phpP*(T163P) (IU1824 was transformed with Δ*gpsB<>aad9* from IU4888 with spontaneous *phpP*(T163P) mutation)	Spc^R, Str^R	This study
IU7797	D39 Δ*cps pbp2a*-HA^4-P_c-*erm* (IU1945 transformed with fusion *pbp2a*-HA^4-P_c-*erm* amplicon	Erm^R	This study
IU7824	D39 Δ*cps* Δ[*spd_1031-1037*]::P_c-*erm* (IU1945 transformed with fusion Δ[*spd_1031-1037*]::P_c-*erm* amplicon)	Erm^R	This study
IU7921-IU7922	D39 Δ*cps* Δ*stkp*::P_c-[*kan-rpsL*$^+$] (IU1945 transformed with fusion Δ*stkp*::P_c-[*kan-rpsL*$^+$] amplicon)	Kan^R	This study
IU7923	D39 Δ*cps* Δ*stkp*::P_c-*erm* (IU1945 transformed with fusion Δ*stkp*::P_c-*erm* amplicon)	Erm^R	This study
IU8224	R6 Δ*gpsB<>aad9* (EL59 transformed with Δ*gpsB<>aad9* amplicon from IU4888)	Spc^R	This study
IU8230	D39 Δ*cps* Δ*gpsB<>aad9//ΔbgaA::kan-t1t2*-P_{fcsk}-*gpsB stkP*-$FLAG^2$-P_c-*erm* (IU4888 transformed with *stkP*-$FLAG^2$-P_c-*erm* from IU7434)	Spc^R, Kan^R, Erm^R	This study
IU8271	D39 Δ*cps* Δ[*spd_1029-1037*]::P_c-[*kan-rpsL*$^+$] (IU7824 transformed with fusion Δ[*spd_1029-1037*]::P_c-[*kan-rpsL*$^+$] amplicon)	Kan^R	This study
IU8311	R6 Δ*gpsB<>aad9 stkP*-$FLAG^2$-P_c-*erm* (IU8224 transformed with *stkP*-$FLAG^2$-P_c-*erm* from IU7434)	Spc^R, Erm^R	This study
IU8369	R6 Δ*gpsB<>aad9* Δ*divIVA*::P_c-[*kan-rpsL*$^+$] (IU8224 transformed with Δ*divIVA*::P_c-[*kan-rpsL*$^+$] from IU3297)	Spc^R, Kan^R	This study
IU8371	R6 Δ*divIVA*::P_c-[*kan-rpsL*$^+$] (EL59 transformed with Δ*divIVA*::P_c-[*kan-rpsL*$^+$] from IU3297)	Kan^R	This study
IU8419	R6 Δ[*phpP-stkP*]::P_c-[*kan-rpsL*$^+$] (EL59 transformed with Δ[*phpP-stkP*]::P_c-[*kan-rpsL*$^+$] amplicon from K739)	Kan^R	This study
IU8496	D39 Δ*cps* Δ*divIVA*::P_c-*erm* (IU1945 transformed with fusion Δ*divIVA*::P_c-*erm* amplicon)	Erm^R	This study
IU8681	D39 Δ*cps rpsL1 ftsZ*-Myc *ezrA*-L-$FLAG^3$-P_c-*erm* (IU7667 transformed with *ezrA*-L-$FLAG^3$-P_c-*erm* from IU5456)	Erm^R, Str^R	This study
IU8805	D39 *rpsL1* Δ*cps phpP*(G229D) (IU7673 transformed with *phpP*(G229D) from IU6442)	Str^R	This study
IU8819	R6 *stkP*-$FLAG^2$-P_c-*erm* (EL59 transformed with *stkP*-$FLAG^2$-P_c-*erm* from IU7434)	Erm^R	This study
IU9256	Rx1	None	(Pozzi *et al*., 1996)
IU9262	Rx1 Δ*gpsB::cat phpP*(L148S) (IU9256	Cm^R	This study (See

	transformed with Δ*gpsB::cat* fusion amplicon, with spontaneous *phpP*(L148S) mutation)		Table S3 for construction)
IU9264	Rx1 Δ*divIVA::erm*	Erm^R	(Fadda *et al.*, 2003)
IU9266	Rx1 Δ*diviVA::erm* Δ*gpsB::cat phpP*(L148S) (IU9262 transformed with Δ*diviVA::erm* amplicon from IU9264)	Cm^R, Erm^R	This study (See Table S3 for construction)
IU9713	D39 Δ*cps rpsL1 ftsZ*-Myc *ezrA*-HA-P_c-*kan* (IU7667 transformed with *ezrA*-HA-P_c-*kan* amplicon from IU6810)	Kan^R, Str^R	This study
IU9767[d]	D39 Δ*cps rpsL1* P_c-[*kan-rpsL*$^+$]-*ftsA*$^+$ IU1824 transformed with P_c-[*kan-rpsL*$^+$]-*ftsA*$^+$ fusion amplicon.	Kan^R	This study
IU9913	D39 Δ*cps divIVA*-HA^2-P_c-*kan* (IU1945 transformed with *divIVA*-HA^2-P_c-*kan* fusion amplicon)	Kan^R	This study
IU9967	D39 Δ*cps rpsL1* HA-*ftsA* (IU9767 transformed with HA-*ftsA* fusion amplicon)	Str^R	This study
U10107	D39 Δ*cps* Δ*gpsB*<>*aad9* Δ[*phpP-stkP*]::P_c-*erm* (E739 Δ[*phpP-stkP*]::P_c-*erm* transformed with Δ*gpsB*<>*aad9* from IU4888)	Spc^R, Erm^R	This study
IU10109	D39 Δ*cps* Δ*gpsB*<>*aad9* Δ*stkP*::P_c-[*kan-rpsL*$^+$] (IU7922 transformed with Δ*gpsB*<>*aad9* from IU4888)	Kan^R , Spc^R	This study
IU10129, IU10138-IU10139, IU10156-IU10157	D39 Δ*cps* Δ*gpsB*<>*aad9*//Δ*bgaA::kan-t1t2-*P_{fcsk}*-gpsB phpP*(G229D) (IU4888 transformed with *phpP(*G229D) from IU6442, without fucose)	Kan^R , Spc^R	This study
IU10180, IU10191	D39 Δ*cps* Δ*gpsB*<>*aad9*//Δ*bgaA::kan-t1t2-*P_{fcsk}*-gpsB phpP*(D192A) (IU4888 transformed with *phpP(*D192A) fusion amplicon, without fucose)	Kan^R , Spc^R	This study
IU10234	D39 Δ*cps rpsL1* HA-*ftsA ftsZ*-P_c-[*kan-rpsL*$^+$] (IU9967 transformed with *ftsZ*-P_c-[*kan-rpsL*$^+$] amplicon from IU7614)	Kan^R, Str^R	This study
IU10302	D39 Δ*cps rpsL1* HA-*ftsA ftsZ*-Myc (IU10234 transformed with *ftsZ*-Myc amplicon from IU7667)	Str^R	This study
IU10349-IU10350, IU10363	D39 Δ*cps* Δ*gpsB*<>*aad9*//Δ*bgaA::kan-t1t2-*P_{fcsk}*-gpsB phpP*(D192A) (IU4888 transformed with *phpP(*D192A) fusion amplicon, without fucose)	Kan^R , Spc^R	This study
IU10423-IU10424	D39 Δ*cps rpsL1 phpP*(G229D) (IU7673 transformed with *phpP*(G229D) from IU6442)	Str^R	This study
IU11183	D39 Δ*phpP*::P_c-*erm* (IU1690 transformed with Δ*phpP*::P_c-*erm* from E736)	Erm^R	This study
IU11187	D39 *rpsL1 phpP*$^+$-P_c-[*kan-rpsL*$^+$]-*stkP*$^+$ (IU1781 transformed with *phpP*$^+$-P_c-[*kan-rpsL*$^+$] from IU7673)	Kan^R	This study
IU11195	D39 *rpsL1 phpP*(G229D) (IU11187	Str^R	This study

	transformed with *phpP*(G229D) from IU6442)		
IU11205	D39 Δ*cps* Δ*gpsB*<>*aad9 phpP*(G229D) Δ*divIVA*::P_c-*erm* (IU6442 transformed with Δ*divIVA*::P_c-*erm* from IU8496)	Spc^R, Erm^R	This study
IU11221	D39 Δ*cps* Δ*gpsB*<>*aad9* Δ*bgaA*::P_c-*erm phpP*(G229D) (IU10129 transformed with Δ*bgaA*::P_c-*erm* amplicon from E46)	Spc^R, Erm^R	This study
IU11223	D39 Δ*cps rpsL1 phpP*(D192A) (IU7673 transformed with *phpP*(D192A) from IU10191)	Str^R	This study
IU11227	D39 *rpsL1 phpP*(D192A) (IU11187 transformed with *phpP*(D192A) from IU10191)	Str^R	This study
IU11238	D39 Δ*cps* Δ*gpsB*<>*aad9* Δ*bgaA*::P_c-*erm phpP*(D192A) (IU10191 transformed with Δ*bgaA*::P_c-*erm* amplicon from E46)	Spc^R, Erm^R	This study
IU11240	D39 Δ*cps rpsL1 phpP*(D192A) (IU7673 transformed with *phpP*(D192A) from IU10191)	Str^R	This study
IU11314	D39 ∆*cps pbp2x*-HA-P_c-*kan gpsB*-L-$FLAG^3$-P_c-*erm* (IU6929 transformed with *gpsB*-L-$FLAG^3$-P_c-*erm* amplicon from IU5458)	Kan^R, Erm^R	This study
IU11316	D39 ∆*cps pbp2b*-HA-P_c-*kan gpsB*-L-$FLAG^3$-P_c-*erm* (IU6933 transformed with *gpsB*-L-$FLAG^3$-P_c-*erm* amplicon from IU5458)	Kan^R, Erm^R	This study
IU11340	D39 Δ*cps rpsL1 ezrA*-L-$FLAG^3$-P_c-*erm* HA-*ftsA ftsZ*-Myc (IU10302 transformed with *ezrA*-L-$FLAG^3$-P_c-*erm* amplicon from IU5456)	Erm^R, Str^R	This study
IU11342	D39 Δ*cps* Δ*gpsB*<>*aad9* Δ*phpP*::P_c-*erm* (E736 transformed with Δ*gpsB*<>*aad9* from IU4888)	Spc^R, Erm^R	This study
IU11344	D39 Δ*cps rpsL1* Δ*gpsB*<>*aad9 phpP*(G229D) (IU8805 transformed with Δ*gpsB*<>*aad9* from IU4888)	Spc^R, Str^R	This study
IU11346	D39 Δ*cps rpsL1* Δ*gpsB*<>*aad9 phpP*(G229D) (IU10423 transformed with Δ*gpsB*<>*aad9* from IU4888)	Spc^R, Str^R	This study
IU11348	D39 Δ*cps rpsL1* Δ*gpsB*<>*aad9 rpsL1 phpP*(D192A) (IU11223 transformed with Δ*gpsB*<>*aad9* from IU4888)	Spc^R, Str^R	This study
IU11350	D39 Δ*gpsB*<>*aad9* Δ*phpP*::P_c-*erm* (IU11183 transformed with Δ*gpsB*<>*aad9* from IU4888)	Spc^R, Erm^R	This study
IU11352	D39 *rpsL1* Δ*gpsB*<>*aad9 phpP*(G229D) (IU11195 transformed with Δ*gpsB*<>*aad9* from IU4888)	Spc^R, Str^R	This study
IU11354	D39 *rpsL1* Δ*gpsB*<>*aad9 phpP*(D192A) (IU11227 transformed with with Δ*gpsB*<>*aad9* from IU4888)	Spc^R, Str^R	This study
IU11412	D39 ∆*cps stkP*-HA-P_c-*kan gpsB*-L-$FLAG^3$-P_c-*erm* (IU7438 transformed with *gpsB*-L-$FLAG^3$-P_c-*erm* amplicon from IU5458)	Kan^R, Erm^R	This study
IU11428	D39 Δ*cps rpsL1 ftsZ*-Myc *ezrA*-HA-P_c-*kan gpsB*-L-$FLAG^3$-P_c-*erm* (IU9713 transformed	Erm^R, Kan^R, Str^R	This Study

	with *gpsB*-L-FLAG^3-P$_c$-*erm* from IU5458)		
IU11432	D39 Δ*cps rpsL1* HA-*ftsA ftsZ*-Myc *gpsB*-L-FLAG^3-P$_c$-*erm* (IU10302 transformed with *gpsB*-L-FLAG^3-P$_c$-*erm* from IU5458)	Erm^R, Str^R	This Study
IU11438	D39 Δ*phpP*::P$_c$-*erm* (IU1690 transformed with Δ*phpP*::P$_c$-*erm* from E736)	Erm^R	This study
IU11442	D39 Δ*cps* Δ*phpP::*P$_c$-*erm* (IU1945 transformed with Δ*phpP*::P$_c$-*erm* from E736)	Erm^R	This study
IU11456	D39 Δ*stkP*::P$_c$-*erm* (IU1690 transformed with Δ*stkP*::P$_c$-*erm* from IU7923)	Erm^R	This study
IU11458, IU11459	D39 Δ[*phpP-stkP*]::P$_c$-*erm* (IU1690 transformed with Δ[*phpP-stkP*]::P$_c$-*erm* from E739)	Erm^R	This study
IU11460	D39 Δ*cps* Δ*stkP*::P$_c$-*erm* (IU1945 transformed with Δ*stkP*::P$_c$-*erm* from IU7923)	Erm^R	This study
IU11462	D39 Δ*cps* Δ[*phpP-stkP*]::P$_c$-*erm* (IU1945 transformed with Δ[*phpP-stkP*]::P$_c$-*erm* from E739)	Erm^R	This study
IU11502	D39 Δ*gpsB*<>*aad9* Δ*phpP*::P$_c$-*erm* (IU11438 transformed with Δ*gpsB*<>*aad9* from IU4888)	Spc^R, Erm^R	This study
IU11504-IU11505	D39 Δ*gpsB*<>*aad9* Δ*stkP*::P$_c$-*erm* (IU11456 transformed with Δ*gpsB*<>*aad9* from IU4888)	Spc^R, Erm^R	This study
IU11506-IU11507	D39 Δ*gpsB*<>*aad9* Δ[*phpP-stkP*]::P$_c$-*erm* (IU11458 transformed with Δ*gpsB*<>*aad9* from IU4888)	Spc^R, Erm^R	This study
IU11508	D39 Δ*cps* Δ*gpsB*<>*aad9* Δ*phpP*::P$_c$-*erm* (IU11442 transformed with Δ*gpsB*<>*aad9* from IU4888)	Spc^R, Erm^R	This study
IU11512	D39 Δ*cps* Δ*gpsB*<>*aad9* Δ[*phpP-stkP*]::P$_c$-*erm* (IU11462 transformed with Δ*gpsB*<>*aad9* from IU4888)	Spc^R, Erm^R	This study
IU11514	D39 Δ*cps divIVA*-Myc-P$_c$-*kan gpsB*-L-FLAG^3-P$_c$-*erm* (IU5458 transformed with *divIVA*-Myc-P$_c$-*kan* fusion amplicon)	Kan^R Erm^R	This study
IU11516	D39 Δ*cps pbp2a*-HA^4-P$_c$-*kan gpsB*-L-FLAG^3-P$_c$-*erm* (IU5458 transformed with *pbp2a*-HA^4-P$_c$-*kan* fusion amplicon)	Kan^R Erm^R	This study
IU11546	D39 Δ*cps* Δ*gpsB*<>*aad9* Δ*stkP*::P$_c$-*erm* (IU11460 transformed with *gpsB*<>*aad9* from IU4888)	Spc^R, Erm^R	This study
IU11558	D39 Δ*cps divIVA*-Myc-P$_c$-*kan* (IU1945 transformed with *divIVA*-Myc-P$_c$-*kan* amplicon from IU11514)	Kan^R	This study
IU11560	D39 Δ*cps pbp2a*-HA^4-P$_c$-*kan* (IU1945 transformed with *pbp2a*-HA^4-P$_c$-*kan* amplicon from IU11516)	Kan^R	This study
IU11566	D39 Δ*cps pbp1a*-HA-P$_c$-*kan gpsB*-L-FLAG^3-P$_c$-*erm* (IU7242 transformed with *gpsB*-L-FLAG^3-P$_c$-*erm* amplicon from IU5458)	Kan^R, Erm^R	This study
IU11574	Rx1 Δ*gpsB*<>*aad9 phpP*$^+$-*stkP*$^+$ (IU9256	Spc^R	This study

	transformed with Δ*gpsB*<>*aad9* from IU4888)		
IU11716	D39 Δ*cps gpsB*-FLAG-P_c-*erm stkP*-HA-P_c-*kan* (IU5838 transformed with *stkP*-HA-P_c-*kan* from IU7438)	Kan^R, Erm^R	This study
IU11955	D39 Δ*cps* Δ*gpsB*<>*aad9 phpP*(R125P) (IU1945 transformed with Δ*gpsB*<>*aad9* from IU4888, with spontaneous *phpP*(R125P) mutation)	Spc^R	This study
IU12059	D39 Δ*cps* Δ*bgaA*::*tet*-P_{Zn}-RBS_{ftsA}-*spd_RS05380* (IU1945 transformed with fusion Δ*bgaA*::P_{Zn}-RBS_{ftsA}-*spd_RS05380*)	Tet^R	This study
K735	D39 Δ*cps* Δ*phpP*::P_c-[*kan-rpsL*$^+$] (IU1945 transformed with fusion Δ*phpP*::P_c-[*kan-rpsL*$^+$] amplicon)	Kan^R	This study
K739	D39 Δ*cps* Δ[*phpP-stkP*]::P_c-[*kan-rpsL*$^+$] (IU1945 transformed with fusion Δ[*phpP-stkP*]::P_c-[*kan-rpsL*$^+$] amplicon)	Kan^R	This study

[a]Strains were constructed as described in *Experimental procedures.* :: indicates an insertion into a region, whereas <> indicates an exact reading frame replacement.

[b]Primers used to synthesize fusion amplicons are listed in Supplemental Tables S2 and S3. All FLAG-tag (FLAG) fusions were made to the carboxyl ends of reading frames. The amino acid sequence of the FLAG epitope is DYKDDDDK (Hopp *et al.*, 1988, Wayne *et al.*, 2010). $FLAG^2$ or $FLAG^3$ indicates two or three tandem sequences of the FLAG epitope, respectively (Waldo *et al.*, 1999, Wayne *et al.*, 2010). L refers to a 10-amino-acid linker sequence (GSAGSAAGSG). The c-Myc epitope amino acid sequence is EQKLISEEDL (Evan *et al.*, 1985), and the HA epitope amino acid sequence is YPYDVPDYA (Tu *et al.*, 1998). See (Land *et al.*, 2013) for additional details.

[c]Antibiotic resistance markers: Erm^R, erythromycin; Cm^R, chloramphenicol, Kan^R, kanamycin; Spc^R, spectinomycin; Tet^R, tetracycline; Str^R, streptomycin.

[d]Details concerning IU9767 construction: The original intergenic region between *spd_1481* and *ftsA* is 218 bp. P_c-[*kan-rpsL*$^+$] cassette is inserted after 70 bp of

intergenic region. After the P_c-[*kan-rpsL*$^+$] cassette is a duplicated 100 bp sequence (30 bp of *spd_1481* and 5' intergenic region). This construct is designed so that the P_c-[*kan-rpsL*$^+$] sequence is followed by 30 bp of 3' *spd_1481* and the entire 218 intergenic region. The duplicated sequence (30 bp of *spd_1481* and 5' intergenic region) terminates transcription of P_c-[*kan-rpsL*$^+$], and maintains the intact intergenic region as promoter sequence for *ftsA*.

TABLE S2. Oligonucleotide primers used for D39 and R6 strains in this study (order follows Table S1)[a]

Primer	Sequence (5' to 3')	Template	Amplicon Product
For construction of E46 (Δ*bgaA*::P_c-*erm*)			
P146	TGGCCATTCATCGCTGGTCGTGCTGAAAT	D39	5' upstream of *bgaA* plus 60 bp of *bgaA*
P148	CATTATCCATTAAAAATCAAACGGATCCTATCCCA CAGCAAACTTACGAATGCTATAAAC		
kanrpsL forward	TAGGATCCGTTTGATTTTTAATGGATAATG	P_c-*erm* cassette	P_c-*erm*
kanrpsL reverse	GGGCCCCTTTCCTTATGCTTTTG		
P149	CAAAAGCATAAGGAAAGGGGCCCGCTCTTCTAGG TTTGAGTGCAGGATTAG	D39	57 bp of *bgaA* + 3' downstream of *bgaA*
P147	TACGCCTTCTATCATGCCTTTGATCGCCCGT		
For construction of E736 (Δ*phpP*::P_c-*erm*)			
P1485	CCAAGCCTTGTTGGAGGCGAATAATTCCCT	D39	5' upstream of *phpP* plus 50 bp of *phpP*
P1486	CATTATCCATTAAAAATCAAACGGATCCTAGACAT AGTCTTGGTTATTTGTTCGTTTCTG		
kanrpsL forward	TAGGATCCGTTTGATTTTTAATGGATAATG	P_c-*erm* cassette	P_c-*erm*
kanrpsL reverse	GGGCCCCTTTCCTTATGCTTTTG		
P1487	CAAAAGCATAAGGAAAGGGGCCCGGAGGTTTAG ACAACATTACGGTTGC	D39	30 bp of *phpP* + 3' downs'tream of *phpP*
TT547	CGGTGCTTGTGGTTGGTAAGTTTCCTCTGT		
For construction of E739 (Δ[*phpP-stkP*]::P_c-*erm*)			
P1485	CCAAGCCTTGTTGGAGGCGAATAATTCCC	D39	5' upstream of *phpP* plus 60 bp of *phpP*
P1486	CATTATCCATTAAAAATCAAACGGATCCTAGACATA GTCTTGGTTATTTGTTCGTTTCTG		
kanrpsL forward	TAGGATCCGTTTGATTTTTAATGGATAATG	P_c-*erm* cassette	P_c-*erm*
kanrpsL reverse	GGGCCCCTTTCCTTATGCTTTTG		
P1497	CAAAAGCATAAGGAAAGGGGCCCAATAAGACTAG AGTCAAGATTTCAATCTACAAACCTA	D39	57 bp of *stkP* and 3' downstream of *stkP*
P1496	CAATACCAAGGCGACAGAAGTTCCTGCCCC		
For construction of IU3297 (Δ*divIVA*::P_c-[*kan-rpsL*$^+$])			
LII-R-015	TGGATAAAGAAGGTAGAAGATAGCTATGCTC	D39	5' upstream region of *divIVA*
SC216	TAACCGTCCAGTTATTATTAAGTAAGTAAGGATCC GTTTGATTTTTAATGGATAATG		
SC215	TAACCGTCCAGTTATTATTAAGTAAGTAAGGATCC GTTTGATTTTTAATGGATAATGTG	P_c-[*kan-rpsL*$^+$] cassette	P_c-[*kan-rpsL*+]
SC218	CTAAACGTCCAAAAGCATAAGGAAAGGGGCCCCT CCAGTGCATCCGACAGGTCCAAC		
SC217	GTCCAAAAGCATAAGGAAAGGGGCCCCTCCAGTG CATCCGACAGGTCCAACACCAGC	D39	3' downstream region of *divIVA*

LII-F-013	CACGTTGGACATGCTATGAACAAGATT		
For construction of IU5456 (*ezrA*-L-FLAG^3-P$_c$-*erm*)			
TT192	ATCGTGTTCCAGCCTTGGTTACGACGCTTT	D39	3' *ezrA*
TT193	CGGAGCCAGCGGAACCAAAACGAATCGTTTCACG TGTTTTC		
AL351	CGATTCGTTTTGGTTCCGCTGGCTCCGCTGC	IU5458	L-FLAG^3-P$_c$-*erm*
TT194	ACACAATAAAATCTTTTTCTTTTATTTCCTCCCGTTA AATAATAGATAACTATTAAAAAT		
TT195	ATAGTTATCTATTATTTAACGGGAGGAAATAAAAGA AAAAGATTTTATTGTGTGAGGAGC	D39	3' downstream of *ezrA*
AL297	GGACCTACTCCTATTGGAGCCCAAC		
For construction of IU6810 (*ezrA*-HA-P$_c$-*kan*)			
TT192	ATCGTGTTCCAGCCTTGGTTACGACGCTTT	D39	3' *ezrA*
SV011	CGGTGATATTCTCATTTTAGCCATGTAATCACTCCT TCTTAATTACAAATTTTTAGCAT		
SV012	AAAATTTGTAATTAAGAAGGAGTGATTACATGGCT AAAATGAGAATATCACCGGA	P$_c$-[*kan*-*rpsL*$^+$] cassette	HA-P$_c$-*kan* with HA added via primer
SV013	ACACAATAAAATCTTTTTCTTCTAAAACAATTCATC CAGTAAAATATAATATTTTATTTT		
SV014	AATATTATATTTTACTGGATGAATTGTTTTAGAAGA AAAAGATTTTATTGTGTGAGGAGC	D39	3' downstream of *ezrA*
TT330	GAGGAGTTCGGACTCGACTCTCTCCTTCAAGAA		
For construction of IU7242 (*pbp1a*-HA-P$_c$-*kan*)			
TT225	AGCCGTGGAAACTCTAAACAAGGTCGGACT	D39	3' *pbp1a*
TT436	GCATAATCTGGAACATCATATGGATATGGTTGTGC TGGTTGAGGATTCTG		
TT437	ATCCTCAACCAGCACAACCATATCCATATGATGTT CCAGATTATGCTTAACC	IU6810	HA-P$_c$-*kan*
TT438	GAAAAATCTGGATGATAAATGCTAAAACAATTCATC CAGTAAAATATAATATTTTATTTT		
TT439	AAATATTATATTTTACTGGATGAATTGTTTTAGCATT TATCATCCAGATTTTTCTGGGTG	D39	3' downstream of *pbp1a*
AL276	CGCGTGCAGAGATTGCCAAGATTGAAGCCTTG		
For construction of IU7644 (*pbp2b*-HA^4-P$_c$-*erm*)			
TT351	AGTTGACGCCTGATTCCTTGGGAACGGTAA	IU7426	3' *pbp2b*-HA^4-P$_c$
TT579	ACAAATTTTGGGCCCGGTTAAGCATAATCTGGAAC ATCATATGGATAAGCATAATCTGGA		
TT435	CCATATGATGTTCCAGATTATGCTTAACCGGGCCC AAAATTTGTTTGATTTG	IU6543	*erm*-plus 3' downstream of *pbp2b*
TT352	TGAAGGACTGGAAAGACCACTGCACCTTCT		
For construction of IU7649 (*phpP*$^+$-P$_c$-[*kan-rpsL*$^+$])			
TT546	AGAGAGTCATCCCGAGTTCGAGCAGGTAAA	D39	3' *phpP* + stop

TT580	CATTATCCATTAAAAATCAAACGGATCCTATCATTC TGCATCCTCCTCGTTCA		codon
kanrpsL forward	TAGGATCCGTTTGATTTTTAATGGATAATG	P_c-[*kan-rpsL*$^+$] cassette	P_c-[*kan-rpsL*$^+$]
kanrpsL reverse	GGGCCCCTTTCCTTATGCTTTTG		
P1487	CAAAAGCATAAGGAAAGGGGCCCGGAGGTTTAGA CAACATTACGGTTGC	D39	60 bp 3' *phpP* + 5' *stkP*
TT547	CGGTGCTTGTGGTTGGTAAGTTTCCTCTGT		
For construction of IU7667 (*ftsZ*-Myc)			
TT165	AGTGGTGCCGATATGGTCTTCATCACTGCT	IU6962	3' *ftsZ* + Myc
TT587	GTATTTTCTTTTACATTCATTTACTTAAAGATCTTCT TCAGAAATAAGTTTTTGTTCACG		
TT588	ACTTATTTCTGAAGAAGATCTTTAAGTAAATGAATG TAAAAGAAAATACAGAACTTGTTT	D39	3' downstream region of *ftsZ*
TT166	TCATTGGGAGAGCCGGTTCCTGTGAAGAAT		
For construction of IU7797 (*pbp2a*-HA^4-P_c-*erm*)			
TT335	CAGGGGGAGTTCGTGGAGTTGTCGGTC	D39	3' fragment of *pbp2a*
SV052	GCATAATCTGGAACATCATATGGATAGCGAAATAG ATTGACTATCGAATCCCA		
SV053	GATTCGATAGTCAATCTATTTCGCTATCCATATGAT GTTCCAGATTATGCTTATCC	IU7644	HA^4-P_c-*erm*
TT338	GCTAGGCTTTGACAAGCATCTTATTTCCTCCCGTT AAATAATAGATAACTATTAAAAAT		
TT339	AGTTATCTATTATTTAACGGGAGGAAATAAGATGC TTGTCAAAGCCTAGCTTTCT	D39	3' downstream region of *pbp2a*
P227	TCTGTTCCCGTGTGATCCGACAAATCCT		
For construction of IU7824 (Δ[*spd_1031-1037*]::P_c-*erm*)			
P396	GCATTCCTAGCACCAATTACCCATCCAGAG	D39	5' upstream of *spd_1037* + 60 bp of 5' *spd_1037*
P398	CATTATCCATTAAAAATCAAACGGATCCTAACAGA CACTTAAAACAAGTGTAGCTACTGA		
kanrpsL forward	TAGGATCCGTTTGATTTTTAATGGATAATG	P_c-*erm* cassette	P_c-*erm*
kanrpsL reverse	GGGCCCCTTTCCTTATGCTTTTG		
P1240	CAAAAGCATAAGGAAAGGGGCCCGCCAAGTTTGT TTATGATGGGGATAAAT	D39	60 bp of 3' *spd_1031* + 3' downstream of *spd_1031*
P1238	TAACGGCACGACGGTCTGATTCCAAACGAA		
For construction of IU7921-7922 (Δ*stkp*::P_c-[*kan-rpsL*]$^+$)			
TT571	GAGCGAGTGCTTGATGCCTGTGCGGCTCCA	D39	5' upstream of *stkP* + 60 bp of *5' stkP*
TT654	CATTATCCATTAAAAATCAAACGGATCCTATCGAC CAATCTGTTTGACAATCCG		
kanrpsL	TAGGATCCGTTTGATTTTTAATGGATAATG	K739	P_c-[*kan-rpsL*$^+$]

forward			plus 3' 60 bp of *stkP* and downstream of *stkP*
P1496	CAATACCAAGGCGACAGAAGTTCCTGCCCC		
For construction of IU7923 (Δ*stkp*::P_c-*erm*)			
TT571	GAGCGAGTGCTTGATGCCTGTGCGGCTCCA	D39	5' upstream of *stkP* + 60 bp of *5' stkP*
TT654	CATTATCCATTAAAAATCAAACGGATCCTATCGAC CAATCTGTTTGACAATCCG		
kanrpsL forward	TAGGATCCGTTTGATTTTTAATGGATAATG	E739	P_c-*erm* plus 3' 60 bp of *stkP* and 3' downstream of *stkP*
P1496	CAATACCAAGGCGACAGAAGTTCCTGCCCC		
For construction of IU8271 (Δ[*spd_1029-1037*]::P_c-[*kan-rpsL*$^+$])			
P396	GCATTCCTAGCACCAATTACCCATCCAGAG	D39	5' upstream of *spd_1037* + 60 bp of 5' *spd_1037*
P398	CATTATCCATTAAAAATCAAACGGATCCTAACAGA CACTTAAAACAAGTGTAGCTACTGA		
kanrpsL forward	TAGGATCCGTTTGATTTTTAATGGATAATG	P_c-[*kan-rpsL*$^+$] cassette	P_c-[*kan-rpsL*$^+$]
kanrpsL reverse	GGGCCCCTTTCCTTATGCTTTTG		
P1512	CAAAAGCATAAGGAAAGGGGCCCCGTTGGCGTTT AACTGTGATTATGAA	D39	60 bp of 3' *spd_1029* + 3' downstream of *spd_1029*
P1510	ACCATTGCCACTGCGAACATGGTCTACAGC		
For construction of IU8496 (Δ*divIVA*::P_c-*erm*)			
TT242	GGGAATGGAATGGATAAAGAAGGTAGAAGA	D39	5' upstream of *divIVA*
SC216	CATTATCCATTAAAAATCAAACGGATCCTTACTTAC TTAATAATAACTGGACGGTTA		
SC215	TAACCGTCCAGTTATTATTAAGTAAGTAAGGATCC GTTTGATTTTTAATGGATAATGTG	P_c-*erm* cassette	P_c-*erm*
SC218	CTAAACGTCCAAAAGCATAAGGAAAGGGGCCCCT CCAGTGCATCCGACAGGTCCAAC		
SC217	GTCCAAAAGCATAAGGAAAGGGGCCCCTCCAGTG CATCCGACAGGTCCAACACCAGC	D39	3' downstream of *divIVA*
TT238	TTCAGCAAGGGCTGACTCAGATGACCATGA		
For construction of IU9767 (P_c-[*kan-rpsL*$^+$]-*ftsA*$^+$)			
TT780	CGCATTACCAAGGAGCAAATAGAGCTTCTTTGGCA GG	D39	3' *spd_1481* + 70 bp intergenic region
TT751	ATTATCCATTAAAAATCAAACGGATCCTATCTATTC AGAAATTCTTATTTTATAAGCTGC		
kanrpsL forward	TAGGATCCGTTTGATTTTTAATGGATAATG	P_c-[*kan-rpsL*$^+$] cassette	P_c-[*kan-rpsL*$^+$]
kanrpsL reverse	GGGCCCCTTTCCTTATGCTTTTG		

TT781	CAAAAGCATAAGGAAAGGGGCCCGCAGAAAAAAT GATTGCAAAGGAAGC	D39	30 bp 3' *spd_1481,* intergenic (281 bp) and 5' *ftsA*
TT753	GCCTTCCGCTAATTTGCGAGAGGTTTTCAA		
For construction of IU9913 (*divIVA*-HA^2-P$_c$-*kan*)			
SC219	TAACCGTCCAGTTATTATTAAGTAAGTGAGGAATA GAATGCCAATTACATCATTAG	D39	3' *divIVA*
AJP116	GCATAATCTGGAACATCATATGGATACTTCTGGTT CTTCATACATTGGGCC		
AJP117	CCCAATGTATGAAGAACCAGAAGTATCCATATGAT GTTCCAGATTATGCTTATC	IU7426	HA^2-P$_c$-*kan*
AJP118	TGTCGGATGCACTGGAGCTACTAAAACAATTCATC CAGTAAAATATAATATTTTATTTT		
AJP119	AATATTATATTTTACTGGATGAATTGTTTTAGTAGC TCCAGTGCATCCGACAGG	D39	3' downstream of *divIVA*
TT238	TTCAGCAAGGGCTGACTCAGATGACCATGA		
For construction of IU9967 (HA-*ftsA*)			
TT750	GGTCATAGGGGGCAATATCTTGACTAAGAAG	D39	5' upstream of *ftsA* +5' *ftsA* with HA sequence added in frame after start codon of *ftsA*
TT765	CTAGCAGCATAATCTGGAACATCATATGGATACAT TACATCGCTTCCTCTCTATCTTCCA		
TT766	TATCCATATGATGTTCCAGATTATGCTGCTAGAGA AGGCTTTTTTACAGGTCTAGATATT	D39	3' *ftsA*
TT753	GCCTTCCGCTAATTTGCGAGAGGTTTTCAA		
For construction of IU11514 (*divIVA*-Myc-P$_c$-*kan*)			
SC219	TAACCGTCCAGTTATTATTAAGTAAGTGAGGAATA GAATGCCAATTACATCATTAG	D39	3' *divIVA*
JC022	TTAAAGATCTTCTTCAGAAATAAGTTTTTGTTCCTT CTGGTTCTTCATACATTGGGCCAA		
JC021	GAACAAAAACTTATTTCTGAAGAAGATCTTTAACCG GGCCCAAAATTTGTTTGATTTGTA	IU9913	Myc-P$_c$-*kan* + *3'* downstream region of *divIVA*
TT238	TTCAGCAAGGGCTGACTCAGATGACCATGA		
For construction of IU11516 (*pbp2a*-HA^4-P$_c$-*kan*)			
TT335b	CAGGGGGAGTTCGTGGAGTTGTCGGTC	IU7797	3' *pbp2a*-HA^4-P$_c$
SV046	CGGTGATATTCTCATTTTAGCCATGTAATCACTCCT TCTTAATTACAAATTTTTAGCAT		
SV047	AAAAATTTGTAATTAAGAAGGAGTGATTACATGGC TAAAATGAGAATATCACCGGA	IU6962	*kan*
AJP218	AAAGCTAGGCTTTGACAAGCATCTTACTAAAACAA TTCATCCAGTAAAATATAATATTTT		
AJP219	TATTATATTTTACTGGATGAATTGTTTTAGTAAGAT GCTTGTCAAAGCCTAGCTTTCTTG	D39	3' downstream of *pbp2a*
P227	TCTGTTCCCGTGTGATCCGACAAATCCT		

For construction of IU12059 (Δ*bgaA*::*tet*-P_{Zn}-RBS_{ftsA}-*spd_RS05380*)			
TT657	CGCCCCAAGTTCATCACCAATGACATCAAC	IU9765 (Tsui *et al.*, 2016)	5' fragment of Δ*bgaA*::*tet*-P_{Zn}-RBS_{ftsA}
BR139	AAGGGATTTTGCTAATCTCTCCAATACATCGCTTC CTCTCTATCTTCCTTGTTATA		
BR138	AGGAAGATAGAGAGGAAGCGATGTATTGGAGAGA TTAGCAAAATCCCTTGG	D39 genomic	*spd_RS05380*
BR141	CAACTGGTTTATGAGAAAGTAAGTTCTTTCATTCTA AACAGTCAATCAAAGGAAGAACTT		
BR140	CTTCCTTTGATTGACTGTTTAGAATGAAAGAACTTA CTTTCTCATAAACCAGTTGCTG	D39 genomic	3' fragment of *bgaA*
CS121	GCTTTCTTGAGGCAATTCACTTGGTGC		
For construction of *phpP*(G229D) strains (*phpP(G229D)*)			
TT546	AGAGAGTCATCCCGAGTTCGAGCAGGTAAA	IU6442	*phpP*(G229D)
TT547	CGGTGCTTGTGGTTGGTAAGTTTCCTCTGT		
For construction of *phpP*(D192A) strains (*phpP*(D192A))			
TT546	AGAGAGTCATCCCGAGTTCGAGCAGGTAAA	IU7673	5' fragment containing *phpP*(D192A)
BR26	CACTGCCTGAAATCATGTTGGTCAAGCCGGCACTA TTGAG		
BR25	TTGCTCAATAGTGCCGGCTTGACCAACATGATTTC A	IU7673	3' fragment containing *phpP*(D192A)-*kanrpsL*
TT574	CGCCTGCTCTGGTGACAAGTAATGAACTGA		
TT546	AGAGAGTCATCCCGAGTTCGAGCAGGTAAA	*phpP* (D192A)	To obtain mutation region for initial cross in
TT580	CATTATCCATTAAAAATCAAACGGATCCTATCATTC TGCATCCTCCTCGTTCA		
TT546	AGAGAGTCATCCCGAGTTCGAGCAGGTAAA	*phpP* (D192A)	To obtain full *phpP*(D192A) for cross ins after sequencing
TT547	CGGTGCTTGTGGTTGGTAAGTTTCCTCTGT		
For construction of K735 (Δ*phpP*::P_c-[*kan-rpsL*$^+$])			
P1485	CCAAGCCTTGTTGGAGGCGAATAATTCCCT	D39	5' upstream of *phpP* plus 5' 60 bp of *phpP*
P1486	CATTATCCATTAAAAATCAAACGGATCCTAGACATA GTCTTGGTTATTTGTTCGTTTCTG		
kanrpsL forward	TAGGATCCGTTTGATTTTTAATGGATAATG	P_c-[*kan-rpsL*$^+$] cassette	P_c-[*kan-rpsL*$^+$]
kanrpsL reverse	GGGCCCCTTTCCTTATGCTTTTG		
P1487	CAAAAGCATAAGGAAAGGGGCCCGGAGGTTTAGA CAACATTACGGTTGC	D39	3' 60 bp of *phpP* + 3' downstream of *phpP*
TT547	CGGTGCTTGTGGTTGGTAAGTTTCCTCTGT		
For construction of K739 (Δ[*phpP-stkP*]::P_c-[*kan-rpsL*$^+$])			

P1485	CCAAGCCTTGTTGGAGGCGAATAATTCCCT	D39	5’ upstream of *phpP* plus 5’ 60 bp of *phpP*
P1486	CATTATCCATTAAAAATCAAACGGATCCTAGACATA GTCTTGGTTATTTGTTCGTTTCTG		
kanrpsL forward	TAGGATCCGTTTGATTTTTAATGGATAATG	P_c-[*kan-rpsL*$^+$] cassette	P_c-[*kan-rpsL*$^+$]
kanrpsL reverse	GGGCCCCTTTCCTTATGCTTTTG		
P1497	CAAAAGCATAAGGAAAGGGGCCCAATAAGACTAG AGTCAAGATTTCAATCTACAAACCTA	D39	3’ 57 bp of *stkP* + 3’ downstream region *of stkP*
P1496	CAATACCAAGGCGACAGAAGTTCCTGCCCC		

[a]Genomic DNA of indicated *S. pneumoniae* strains was used as templates for PCR reactions. Strain genotypes are listed in Table S1.

TABLE S3. Oligonucleotide primers for Rx1 strains used in this study[a]

Primer		
*ypsB*_KOF1_177[a]	GGGTGTCTTGGCTTGTGTTTA	Δ*gpsB* in Rx1
*ypsB*_KOR2_709[a]	TCAAACAAATTTTCATCAAGCTTGACC TCACGTCCAAACTCTT	Δ*gpsB* in Rx1
*ypsB*_KOF3_690[a]	AAGAGTTTGGACGTGAGGTCAAGCTT GATGAAAATTTGTTTGA	Δ*gpsB* in Rx1
*ypsB*_KOR4_933[a]	TCCAATCTATTCAGGCGTTTCTCTAGA ACTAGTGGATCCCCCGG	Δ*gpsB* in Rx1
*ypsB*_KOF5_913[a]	CCGGGGGATCCACTAGTTCTAGAGAA ACGCCTGAATAGATTGGA	Δ*gpsB* in Rx1
*ypsB*_KOR6_1585[a]	TTGAAAACGAACACGTCCATC	Δ*gpsB* in Rx1
LN235[a]	AGTGTGAGAAAATTTGGT	*primer forward*, amplification *divIVA::erm* from Δ*divIVA* (Fadda *et al*., 2003)
LN236[a]	CGCTGGGAATATAAGGAT	*primer reverse*, amplification *divIVA::erm* from Δ*divIVA* (Fadda *et al*., 2003)
AM61F[b]	GACTGTATCAAGCTAGAACGGTTAAG	*primer forward,* PCR verification of *spr1061-spr1060* (*spd_1038-spd_1037*)
AM59R[b]	GAGTAATCCTGATGAGAATGATCCAG	*primer reverse,* PCR verification of *spr1061-spr1060* (*spd_1038-spd_1037*)
TT575[b]	AATCAGAAAGGGATTGCTTTATGCAGT TCC	*primer forward,* PCR verification of *spr1057-spr1056* (*spd_1034-spd_1033*)
TT578[b]	CTCCCATACAGCCATTACGATTCATAT TGA	*primer reverse,* PCR verification of *spr1057-spr1056* (*spd_1034-spd_1033*)
TT635[b]	GCCTTTATGAGGCACCTAAGGGGTAT AGTC	*primer forward,* PCR verification of *spr1060-spr1053* (*spd_1037-spd_1030*)
P1238[b]	TAACGGCACGACGGTCTGATTCCAAA CGAA	*primer reverse,* PCR verification of *spr1060-spr1053* (*spd_1037-spd_1030*)

P1481[b]	TTATGTAGGAGGAACCGAGGGCGGAGGAAT	*primer forward,* PCR verification of *spr1059-spr1056* (*spd_1036-spd_1033*)
P1482[b]	AGACGAGTGTTCCATAGCCGACTCCTTCATTT	*primer reverse,* PCR verification of *spr1059-spr1056* (*spd_1036-spd_1033*)
pKNT25/pUT18_*gpsB*_PF[c]	AACTGCAGGATGGCAAGTATTATTTTTTCAGCG	*primer forward*, PCR amplification of *gpsB* for plasmid insert for B2H studies
pKNT25/pUT18_*gpsB*_BR[c]	CGGGATCCTCAAAATCTGAGTTATCTAAAATTTG	*primer reverse*, PCR amplification of *gpsB* for plasmid insert for B2H studies
pKNT25/pUT18-*divIVA*_PF[c]	AACTGCAGGATGCCAATTACATCATTAGAAATA	*primer forward*, PCR amplification of *divIVA* for plasmid insert for B2H studies
pKNT2/pUT18-*divIVA*_BR[c]	CGGGATCCTTCTGGTTCTTCATACATTGGG	*primer reverse*, PCR amplification of *divIVA* for plasmid insert for B2H studies
pKNT25/pUT18_*ezrA*_PF[c]	AACTGCAGGATGTCTAATGGACAAC	*primer forward*, PCR amplification of *ezrA* for plasmid insert for B2H studies
pKNT25/pUT18_*ezrA*_BR[c]	CGGGATCCTCAAAACGAATCGTTTCA	*primer reverse*, PCR amplification of *ezrA* for plasmid insert for B2H studies
pKNT25/pUT18_*ftsZ*_PF[c]	AACTGCAGGATGACATTTTCATTTGATACAGCTG	*primer forward*, PCR amplification of *ftsZ* for plasmid insert for B2H studies
pKNT25/pUT18_*ftsZ* _BR[c]	CGGGATCCCGATTTTTGAAAAATGGAGGTGTA	*primer reverse*, PCR amplification of *ftsZ* for plasmid insert for B2H studies
pKNT25/pUT18_*stkP*_BF[c]	CGGGATCCCATGATCCAAATCGGC	*primer forward*, PCR amplification of *stkP* for plasmid insert for B2H studies
pKNT25/pUT18_*stkP*_ER[c]	CGGAATTCGAAGGAGTAGCTGAAGTT	*primer reverse*, PCR amplification of *stkP* for

		plasmid insert for B2H studies
pKNT25/pUT18_49F[d]	CGCAATTAATGTGAGTTAGC	*primer forward, sequencing pKNT25/pUT18*
pKNT25_328R[d]	TTGATGCCATCGAGTACG	*primer reverse, sequencing pKNT25*
pUT18_304R[d]	CGAGCGATTTTCCACAACAA	*primer reverse, sequencing pUT18*

[a]Genomic DNA of the Rx1 *S. pneumoniae* strains was used as templates for PCR reactions. Strain genotypes are listed in Table S1.

[b]Indicates primers used to verify by PCR the arrangement of *spd_1033-spd_1038* chromosomal region of Rx1.

[c]Indicates primers used to obtain gene sequences for B2H studies.

[d]Indicates primers to verify the correct sequence of the genes cloned in the B2H vectors.

TABLE S4. PhpP model similarity to known protein structures.

Organism	Protein function	PDB ID	RMSD[a]	Z-score[b]
S. agalactiae (Stp1) AA 1-242	Ser/Thr protein phosphatase	2PK0	0.4	44.2
M. tuberculosis (Mspp) AA 1-233	Ser/Thr protein phosphatase	2V06	1.3	29.1
M. tuberculosis (PstP) AA 1-240	Ser/Thr protein phosphatase	1TXO	1.4	30.5

[a]RMSD was determined via PyMOL alignment (AA 1-246 of PhpP) (Schrodinger) of the PDB modelling file generated from Phyre2 input of PhpP sequence (Kelley *et al.*, 2015). See *Experimental procedures* for details.

[b]Z-score was determined via input of the PhpP PDB modeling file generated from Phyre2 into DALI server (Kelley *et al.*, 2015, Holm & Rosenstrom, 2010).

TABLE S5. Relative protein phosphorylation levels in mutant strains compared to those in the Rx1 and R6 parent laboratory strains[a]

Strain Number	Genotype	Sample OD_{620}	Relative phosphorylation of StkP/MapZ[b]	Relative phosphorylation of DivIVA
IU9256	Rx1	0.4	≡1	≡1
IU9262	Rx1 Δ*gpsB* *phpP*(L148S) *sup4*	0.4	1.2 ± 0.2	1.2 ± 0.4
IU11574	Rx1 Δ*gpsB*	0.4	0.2 ± 0.2	0.3 ± 0.2
EL59	R6	0.4	≡1	≡1
IU8224	R6 Δ*gpsB*	0.4	0.6 ± 0.2	0.2 ± 0.2
IU8419	R6 Δ[*phpP-stkP*]::P_c-[*kan-rpsL*$^+$]	0.4	0.1 ± 0.1	0.1 ± 0.06

[a]Relative protein phosphorylation levels are listed for mutants compared to the Rx1 and R6 parent laboratory strains grown exponentially to OD_{620} ≈ 0.4. Protein phosphorylation was determined as described in *Experimental procedures*, and a representative Western blot with the same sample order is shown in Figure 2A, where StkP~P/MapZ~P corresponds to the double band at ≈ 70 kDa, and DivIVA~P corresponds to the band around ≈ 45 kDa. The phosphorylation levels are the mean (±SEM) from at least two independent experiments.

[b]The signal level for strains IU9262, IU8224, and IU8419 was low and near the background level. We do not know why StkP/MapZ phosphorylation was greater in the R6 Δ*gpsB* mutant IU8224 than in the Rx1 Δ*gpsB* mutant IU9262; however, the R6 Δ*gpsB* mutant grew much better than the Rx1 Δ*gpsB* mutant, reflective of genetic differences between these two laboratory strains (see Table 1; *Results*).

TABLE S6. Depletion of GpsB in the D39 background leads to decrease in phosphorylation.[a]

Strain Number	Genotype	Sample OD_{620}	Relative phosphorylation of StkP/MapZ	Relative phosphorylation of DivIVA
IU4888	Δ*gpsB* P_{fcsK}-*gpsB* +fucose, 1 h	0.1	0.9 ± 0.2	0.7 ± 0.1
IU4888	Δ*gpsB* P_{fcsK}-*gpsB* +fucose, 3 h	0.2-0.4	1.7 ± 0.2	1.6 ± 0.1
IU1945	D39 Δ*cps* parent	0.1	≡1	≡1
IU1945	D39 Δ*cps* parent	0.2-0.4	1.5 ± 0.1	1.6 ± 0.1
E739	Δ[*phpP-stkP*]::P_c-*erm*	0.1	0	0
E739	Δ[*phpP-stkP*]::P_c-*erm*	0.2-0.4	0	0
IU4888	Δ*gpsB* P_{fcsK}-*gpsB* –fucose, 1 h	0.1	0.2 ± 0.1	0.2 ± 0.1
IU4888	Δ*gpsB* P_{fcsK}-*gpsB* –fucose, 2 h	0.2	0.5 ± 0.1	0.4 ± 0.1
IU4888	Δ*gpsB* P_{fcsK}-*gpsB* –fucose, 3 h	0.2-0.3	0.5 ± 0.2	0.4 ± 0.2

[a]Relative protein phosphorylation levels are listed for merodiploid strains depleted for GpsB (-fucose) or not depleted for GpsB (+fucose) for the times indicated compared to the exponentially growing IU1945 parent strain. Samples were taken at the OD_{620} values indicated. Protein phosphorylation was determined as described in *Experimental procedures*, and a representative Western blot with the same sample order is shown in Figure 2B, where StkP~P/MapZ~P corresponds to the double band at ≈ 70 kDa, and DivIVA~P corresponds to the band around ≈ 45 kDa. The relative phosphorylation levels are based on means (±SEM) from at least three independent experiments. Signal levels <0.2 are at the level of background detection of this method and cannot be accurately quantitated.

TABLE S7. Relative protein phosphorylation levels in unencapsulated D39 Δ*gpsB* original and reconstructed suppressor strains[a]

Strain Number	Genotype	Sample OD_{620}	Relative phosphorylation of StkP/MapZ	Relative phosphorylation of for DivIVA
IU1945	D39 Δ*cps*	0.4	≡1	≡1
IU5845[b]	Δ*gpsB* (*sup2*)	0.4	0.2 ± 0.02	0.2 ± 0.1
IU6441[b]	Δ*gpsB* (*sup3*)	0.4	0.1 ± 0.01	0.1 ± 0.03
IU6442[b]	Δ*gpsB* (*sup1*) *phpP*(G229D)	0.4	1.2 ± 0.04	1.2 ± 0.1
E46[c]	D39 Δ*cps* Δ*bgaA*::P_c-*erm*	0.4	0.8 ± 0.2	0.8 ± 0.1
IU11221[d]	D39 Δ*cps* Δ*gpsB* *phpP*(G229D) Δ*bgaA*::P_c-*erm*	0.4	1.1 ± 0.3	1.2 ± 0.1
IU11442[e]	D39 Δ*cps* Δ*phpP*::P_c-*erm*	0.4	0.4 ± 0.1	1.1 ± 0.1
IU11460[f]	D39 Δ*cps* Δ*stkP*::P_c-*erm*	0.4	0.1 ± 0.02	0.1 ± 0.01
IU11462[f]	D39 Δ*cps* Δ[*phpP-stkP*]::P_c-*erm*	0.4	0.04 ± 0.02	0.1 ± 0.03

[a]Relative protein phosphorylation levels are listed for mutants compared to the unencapsulated derivative of D39 (IU1945) grown exponentially to OD_{620} ≈ 0.4. Protein phosphorylation was determined as described in *Experimental procedures*, and a representative Western blot with the same sample order is shown in Figure 3, where StkP~P/MapZ~P corresponds to the double band at ≈ 70 kDa, and DivIVA~P corresponds to the band around ≈ 45 kDa. Phosphorylation levels are the mean (±SEM) from at least two independent experiments. Signal levels <0.2 are at the level of background detection of this method and cannot be accurately quantitated.

[b]Originally isolated Δ*gpsB* suppressor strain described in Table 2.

[c]Isogenic parent strain for reconstructed Δ*gpsB phpP*(G229D) (*sup1*) strain in Fig. 3.

[d]Reconstructed Δ*gpsB phpP*(G229D) (*sup1*) mutant (see Fig. 3 and Fig. 4).

[e]The Δ*phpP*::P_c-*erm* mutation is polar on downstream StkP kinase expression resulting in decreased phosphorylation of the StkP/MapZ proteins. See text and Fig. 3 for details.

[f]Negative control strains lacking the StkP protein kinase.

TABLE S8. Genes deleted and duplicated in the IU5845 (*sup2*) Δ*gpsB* unencapsulated D39 suppressor strain[a]

Region	Gene	Putative or defined function
Genes in large Δ[*spd_1026-spd_1037*] deletion	*spd_1026*	Branched chain alpha-keto acid dehydrogenase subunit E2
	spd_1027	TPP-dependent acetoin dehydrogenase complex, E1 protein subunit beta
	spd_1028	Pyruvate dehydrogenase E1 subunit alpha
	spd_1029	Multidrug resistance protein NorM
	spd_RS05480	Hypothetical protein, no BLAST similarity to proteins of known function
	spd_1030	*pyrC*, dihydroorotase
	spd_1031	*mutX*, *8-oxo-dGTP diphosphatase*
	spd_1032	*ung*, uracil-DNA glycosylase
	spd_1033	Hypothetical protein, uncharacterized, no BLAST similarity to proteins of known function
	spd_1034	Non-canonical pyrimidine nucleotidase, HAD-like superfamily domain (YjjG)
	spd_1035	Hypothetical protein, BLAST to phosphate dependent mannose transporter
	spd_1036	PTS fructose transporter subunit IIA
	spd_1037	Hypothetical protein, BLAST to histidine triad protein
Selected genes in large 134 gene duplication Ω[*spd_0889-spd_1026*][b]	*spd_0888*	Adhesion protein, BLAST to AdcA
	spd_0889	Hypothetical protein, BLAST to histidine triad proteins, HIT family hydrolases
	spd_0904	Thymidine kinase, predicted
	spd_0925	Hydrolase, predicted, BLAST to ADP-ribosylglycohydrolase
	spd_0926	Lipid kinase, predicted
	spd_0939	MutR family transcriptional regulator, predicted
	spd_0952	FtsW
	spd_0953	Phosphoenolpyruvate carboxylase
	spd_0958	RNA polymerase sigma factor SigA
	spd_0973	ATP-dependent DNA helicase PcrA
	spd_0981	Adenylate cyclase, predicted
	spd_0982	GTP pyrophosphokinase, predicted
	spd_0983	NAD(+) kinase, predicted
	spd_0985	*eutD*, phosphate acetyltransferase
	spd_0999	MutR family transcriptional regulator, predicted
	spd_1001	*ligA*, DNA ligase (NAD^+) LigA

	***spd_RS05380* (before *spd_1011*)**	**Phosphoserine phosphatase, predicted**
	spd_1018	Immunoglobulin A1 protease

[a]See Table 2 for suppressor isolation and Figure S3 for a depiction of the Δ[*spd_1026-spd_1037*] Ω[*spd_0889-spd_1026*] in the *spd_1034* region of the pneumococcal chromosome of strain IU5845. The deletion and insertion in the IU6441 (*sup3*) suppressor strain overlap and are slightly smaller than those listed above (see Fig. S3B).

[b]Genes were selected based on functions important for cell division, normal growth, pneumococcal pathogenesis, or putative roles in protein phosphorylation. The mechanisms, if any, by which the duplications contribute to Δ*gpsB* suppression and the steps that lead to formation of the deletions/insertions are unknown.

SUPPLEMENTAL FIGURE LEGENDS

Fig. S1. Δ*divIVA* mutations are not epistatic to Δ*gpsB* in pneumococcal strain Rx1. A) Representative growth curve of Rx1 strains. Strains are listed, 1-4 as follows: 1, Rx1 (IU9256); 2, Rx1 Δ*gpsB phpP*(L148S) (IU9262); 3, Rx1 Δ*divIVA* (IU9264); 4, R6 Δ*gpsB phpP*(L148S) Δ*divIVA* (IU9266). Doubling times were calculated using a nonlinear regression exponential growth curve program (GraphPad Prism) for OD_{620} ≈ 0.015 to 0.25. B) FDAA staining and microscopy of Rx1 live cells were performed as described in *Experimental procedures*. The panels from left to right are: phase, FDAA labeling, and phase/FDAA overlay. Representative images are shown of ≥95% of the cells (n>50) examined manually of each strain. The experiments were performed two to three times independently with similar results. Reduced autolysis of the R6 Δ*gpsB phpP*(L148S) Δ*divIVA* (IU9266) mutant in stationary phase was observed in each experiment.

Fig. S2. A) Diagram of the chromosomal *phpP-stkP* operon with surrounding genes. The positions of mutations that lead to the G117D, L148S, T163P, D192A, and G229D amino acid changes in PhpP are indicated, together with the location of the *stkP*(G10 *STOP*) mutation in one of the constructed *phpP*(G229D) mutants. B) Diagram showing the intermediate *phpP*$^+$-[P_c-*kanrpsL*$^+$]-*stkP*$^+$ strain used to construct *phpP*(G229D) or *phpP*(D192A) mutants in the *rpsL1* background. Primers TT546 and TT547 were used to amplify *phpP*$^+$-[P_c-*kanrpsL*$^+$]-*stkP*$^+$, *phpP*(G229D), or *phpP*(D192A) for transformations.

Fig. S3. A) Diagram of the chromosomal locus indicating the deletion/duplication mutations found in the D39 Δ*cps* Δ*gpsB sup2* (IU5845) and *sup3* (IU6441) suppressor strains (Table 2, lines 2 and 3). IU5845 has a deletion of Δ*spd*_[*1026-1037*] and a

duplication of Ω*spd_*[*0889-1026*] (indicated in figure), while IU6441 has a deletion of Δ*spd_*[*1029-1037*] and a duplication of Ω*spd_*[*0889-1024*] (see B, below). See Table S8 for a list of deleted genes and selected duplicated genes in the *sup2* and *sup3* Δ*gpsB* suppressor strains. In addition, mutations are indicated in this region that are present in laboratory strain Rx1 or R6 parent compared to the D39 Δ*cps* progenitor strain. The deletions at the bottom were constructed in the D39 Δ*cps* strain and tested for their effects on protein phosphorylation (Fig. S8). B) MiSeq DNA read distribution showing chromosomal duplications and deletions in the *spd_1034* region of the genomes of Δ*gpsB sup3* (IU6441) and Δ*gpsB sup2* (IU5845) that are not present in Δ*gpsB sup1* (IU6442) (see Table 2, rows 1-3).

Fig. S4. Structure and specific activity of wild-type and mutant *Spn* PhpP proteins. A) Threaded structure of the pneumococcal PhpP protein phosphatase showing amino acids in the active site region changed in Δ*gpsB* suppressor mutants (see Table 2). Phyre2 modeling of *Spn* PhpP structure (blue) is overlaid with the *S. agalactiae* Stp1 structure (green), PDB ID: 2PK0. Alignment was performed using PyMOL (Schrödinger, LLC). Inset shows a close up of the aligned structure where the *Spn* active site arginine (R13), and amino acid changes found in Δ*gpsB* suppressor mutants are indicated as pink sticks at residues G117, L148, T163, G229, R13 (active site arginine) (Rantanen *et al.*, 2007), and D192 (aspartate residue important for binding Mn^{2+} ions required for PhpP activity) (Nováková *et al.*, 2005). B) Phosphatase specific activities of purified PhpP(G229D) and PhpP(L148S) are greatly reduced (>16-fold) compared to wild-type $PhpP^{+}$. Phosphatase activity was quantified as pmol of free phosphate released in a defined time from phosphorylated peptide RRA(pT)VA by purified His-tagged PhpP

protein as described previously (Nováková *et al.*, 2005). The PhpP(G229D) and PhpP(L148S) amino acid changes were introduced into expression plasmid pEXPhpP^{+} by using the QuickChange mutagenesis kit (Stratagene) and the following primers: PhpP_G229D_F GTTTTGCTAACAATGCAGGAGATTTAGACAACATTACGGTTGC; PhpP_G229D_RGCAACCGTAATGTTGTCTAAATCTCCTGCATTGTTAGCAAAAC; PhpP_G229D_RGCAACCGTAATGTTGTCTAAATCTCCTGCATTGTTAGCAAAAC; and PhpP_G229D_R GCAACCGTAATGTTGTCTAAATCTCCTGCATTGTTAGCAAAAC. Mutations in expression plasmids were confirmed by DNA sequencing. Phosphate-release assays using the malachite green phosphate-release kit (POMG-25H; BioAssay Systems, Hayward, CA) were performed twice independently for each purified protein. Data shown are mean ± SEM.

Fig. S5. Changes in PhpP suppressors are at conserved amino acids. Degree of conservation of each residue in *Spn* PhpP and *S. agalactiae* PP2C phosphatase is shown, as indicated by the legend in the bottom right corner. Asterisks mark essential Mn^{2+} coordinating and catalytic residues D192 and R13 (Nováková *et al.*, 2005, Rantanen *et al.*, 2007), and residues found to be mutated in Δ*gpsB* suppressor strains: G117, R125, L148, T163, and G229. Degree of conservation is indicated by color coded boxes, which was determined by the ConSurf server (Ashkenazy *et al.*, 2016) using a multisequence alignment of the amino acid sequences from the *S. agalactiae* PP2C phosphatase, *S. pneumoniae* PhpP, and homologs *L. monocytogenes* Stp, *B. subitlis* PrpC, *P. aeruginosa* Stp1, and *S. mutans* Pppl.

Fig. S6 Western blot demonstrating that PhpP(D192A) and PhpP(G229D) amino acid changes do not significantly affect StkP and PhpP amounts in reconstructed

suppressor strains. Strains were harvested at OD_{620} ≈ 0.4. A) Immunoblotting was performed with α-PhpP antibody for the following strains: lane 1, wild-type parent D39 Δ*cps rpsL1* (IU1824); and lane 2, D39 Δ*cps rpsL1* Δ*gpsB phpP*(D192A) (IU11348). B) Immunoblotting of the same blot was performed with α-StkP antibody. C) Immunoblotting was performed with α-PhpP antibody for the following strains: lane 1, wild-type parent D39 Δ*cps* (IU1945); and lane 2, D39 Δ*cps* Δ*gpsB* Δ*bgaA*::P_c-*erm phpP*(G229D) (IU11221). D) Immunoblotting of the same blot was performed with α-StkP antibody. These experiments were performed twice independently with similar results.

Fig. S7. Western blot demonstrating that the PhpP(G229D) amino acid change does not affect PhpP or StkP amounts in the originally isolated Δ*gpsB sup1* strain (Table 2, line 1). Strains were harvested at OD_{620} ≈ 0.4. A) Immunoblotting was performed with α-PhpP antibody on the following strains: lane 1, wild-type parent D39 Δ*cps* (IU1945); lane 2, D39 Δ*cps ΔgpsB phpP*(G229D) (IU6442, *sup1*); lane 3, D39 Δ*cps rpsL1 phpP*(G229D) *stkP* (G10 *STOP*) (IU7685); lane 4, D39 Δ*cps* Δ[*phpP-stkP*] (K739) control; lane 5, D39 Δ*cps* Δ*stkP* (IU7921); and lane 6, D39 Δ*cps* Δ*phpP* (K735) control. B) Immunoblotting of the same blot was performed with α-StkP antibody. These experiments were performed three times independently with similar results. The red line marks a colored 53 kDa standard that did not transfer.

Fig. S8. Deletion of *spd_*[*1029-1037*] does not affect threonine phosphorylation of proteins. Western blotting using α-pThr antibody was used to detect proteins phosphorylated at Thr residues in strains containing either the *spd_*[*1029-1037*] or *spd_*[*1031-1037*] deletion harvested at OD_{620} ≈ 0.1 and 0.4. Lanes 1 and 5, wild-type

parent D39 Δ*cps* (IU1945); lanes 2 and 6, D39 Δ*cps* Δ[*spd_1031-1037*]::P_c-*erm* (IU7824); lanes 3 and 7, D39 Δ*cps* Δ[*spd_1029-1037*]::P_c-[*kan-rpsL*$^+$] (IU8271); and lanes 4 and 8, D39 Δ*cps* Δ[*phpP-stkP*] (E739) control. This experiment was performed three times with similar results. More protein phosphorylation was routinely detected in cells at higher density (0.4) than at lower density (0.1). The red line marks a colored 53 kDa standard that did not transfer.

Fig. S9. GpsB is not required for localization of StkP in rings in laboratory strain Rx1. Fluorescence microscopy was performed on the Rx1 parent and Rx1 Δ*gpsB phpP*(L148S) derivative strains expressing P_{Zn}-*gfp-stkP*$^+$*.* Cells were inoculated 1:100 from frozen glycerol starters (OD_{620} ≈ 0.3) in pre-warmed BHI broth and incubated at 37°C until they reached OD_{620}=0.1. At this time, cultures were split into two tubes containing no added zinc or 0.65 mM $ZnCl_2$ and incubated at 37°C. Growth was monitored turbidimetrically every 30 min and samples for microscopy were taken. A) Rx1 parent strain expressing GFP-StkP ectopically; and B) Rx1 Δ*gpsB phpP*(L148S) expressing GFP-StkP ectopically, taken after two hours after induction. Percentage of cells with StkP rings is based on 142 manually examined cells of the Δ*gpsB phpP*(L148S) mutant.

Fig. S10. Pairwise co-IP of GpsB-L-FLAG[3] with bPBP2b-HA, StkP-HA, or aPBP2a-HA[4], but not with bPBP2x-HA. Co-IP experiments were performed as described in *Experimental procedures.* A) Western blots of cell lysates before co-IP was performed. Total protein loaded for each sample was 62 µg. The top blot was probed with anti-HA primary antibody, and the bottom blot was probed with anti-FLAG primary antibody. Predicted molecular weights (MWs) of bPBP2x-HA, bPBP2b-HA, StkP-HA, and

aPBP2a-HA[4] are 83.5 kDa, 75.7 kDa, 73.5 kDa, and 85.2 kDa, respectively. The predicted MW of GpsB-L-FLAG[3] monomer is 16.4 kDa. B) Western blot after co-IP was performed. Total amount of elution loaded was 20 µL after mixing 1:1 with 2X Laemmli sample buffer. The top blot was probed with anti-HA primary antibody for detection of HA tagged prey proteins, using GpsB-L-FLAG[3] as bait. Predicted MWs of proteins are listed in A. The bottom blot was probed with anti-FLAG primary antibody for detection of GpsB-L-FLAG[3]. Two major bands can be detected by anti-FLAG primary antibody in the strains expressing GpsB-L-FLAG[3]; the bottom band is the monomer and the upper band may be a trimer. Strains used to prepare extracts were constructed in D39 Δ*cps* strain IU1945. Lane 1 *pbp2x*-HA *gpsB*$^+$ (IU6929); lane 2 *gpsB*-L-FLAG[3] *pbp2x*-HA (IU11314); lane 3 *pbp2b*-HA *gpsB*$^+$ (IU6933); lane 4 *gpsB*-L-FLAG[3] *pbp2b*-HA (IU11316); lane 5 *stkP*-HA *gpsB*$^+$ (IU7438); lane 6 *gpsB*-L-FLAG[3] *stkP*-HA (IU11412); lane 7 *pbp2a*-HA[4] *gpsB*$^+$ (IU11560); and lane 8 *pbp2a*-HA[4] *gpsB*-L-FLAG[3] (IU11516).

Fig. S11. Pairwise co-IP of GpsB-L-FLAG[3] with EzrA-HA, but not with HA-FtsA or aPBP1a-HA. Co-IP experiments were performed as described in *Experimental procedures*. A) Western blots of cell lysates before co-IP was performed. Total protein loaded for each sample was 57 µg. The top blot was probed with anti-HA primary antibody, and the bottom blot was probed with anti-FLAG primary antibody. Predicted molecular weights (MWs) of EzrA-HA, HA-FtsA, and aPBP1a-HA are 67.6 kDa**,** 50.7 kDa, and 81.0 kDa, respectively. The predicted MW of GpsB-L-FLAG[3] monomer is 16.4 kDa. B) Western blot after co-IP was performed. Total amount of elution loaded was 20 µL after mixing 1:1 with 2X Laemmli sample buffer. The top blot shown was probed with anti-HA primary antibody for detection of HA tagged prey proteins, using GpsB-L-FLAG[3]

as bait. Predicted MWs of proteins are listed in A. The bottom blot was probed with anti-FLAG primary antibody for GpsB-L-FLAG^3. Two major bands can be detected by anti-FLAG primary antibody in the strains expressing GpsB-L-FLAG^3; the bottom band is the monomer and the upper band may be a trimer. Strains used to prepare extracts were constructed in D39 Δ*cps* strain IU1945. Lane 1, *ezrA*-HA *ftsZ*-Myc *gpsB*$^+$ (IU9713); lane 2, *gpsB*-L-FLAG^3 *ezrA*-HA *ftsZ*-Myc (IU11428); lane 3, HA-*ftsA ftsZ*-Myc *gpsB*$^+$ (IU10302); lane 4, *gpsB*-L-FLAG^3 HA-*ftsA ftsZ*-Myc (IU11432); lane 5, *pbp1a*-HA *gpsB*$^+$ (IU7242); and lane 6 *gpsB*-L-FLAG^3 *pbp1a*-HA (IU11566).

Fig. S12. Pairwise co-IP of EzrA-L-FLAG^3 with FtsZ-Myc, but lack of pairwise co-IP of GpsB-L-FLAG^3 with DivIVA-Myc or FtsZ-Myc. Co-IP experiments were performed as described in *Experimental procedures*. A) Western blots of cell lysates before co-IP was performed. Total protein loaded for each sample was 69 µg. The top blot was probed with anti-Myc primary antibody, and the bottom blot was probed with anti-FLAG primary antibody. Predicted molecular weights (MWs) of DivIVA-Myc and FtsZ-Myc are 31.5 kDa and 45.7 kDa, respectively. DivIVA was previously shown to run at a higher MW than predicted (45 kDa) (Fadda *et al.*, 2007). The predicted MWs of GpsB-L-FLAG^3 and EzrA-L-FLAG^3 are 16.4 kDa and 70.3 kDa, respectively. B) Western blot after co-IP was performed. Total amount of elution loaded was 20 µL after mixing 1:1 with 2X Laemmli sample buffer. The top blot was probed with anti-Myc primary antibody for detection of Myc tagged prey proteins, using GpsB-L-FLAG^3 or EzrA-L-FLAG^3 as bait. Predicted MWs of proteins are listed in A. The bottom blot was probed with anti-FLAG primary antibody for GpsB-L-FLAG^3 or EzrA-L-FLAG^3. Strains used to prepare extracts were constructed in D39 Δ*cps* strain IU1945. Lane 1, *divIVA*-Myc *gpsB*$^+$ (IU11558); lane 2

gpsB-L-FLAG^3 *divIVA*-Myc (IU11514); lane 3, HA-*ftsA ftsZ*-Myc *gpsB*$^+$ (IU10302); lane 4, *gpsB*-L-FLAG^3 HA-*ftsA ftsZ*-Myc (IU11432); lane 5, HA-*ftsA ftsZ*-Myc *ezrA*$^+$ (IU10302); lane, 6 HA-*ftsA ftsZ*-Myc *ezrA*-L-FLAG^3 (IU11340).

Fig. S13. Pairwise co-IP of StkP-FLAG^2 with bPBP2x-HA and bPBP2b-HA. Co-IP experiments were performed as described in *Experimental procedures*. A) Western blots of cell lysates before co-IP was performed. Total protein loaded for each sample was 52 µg. The top blot was probed with anti-HA primary antibody, and the bottom blot was probed with anti-FLAG primary antibody. Predicted molecular weights (MWs) of bPBP2x-HA and bPBP2b-HA are 83.5 kDa and 75.7 kDa, respectively. Predicted MW of StkP-FLAG^2 is 74.3 kDa. B) Western blot after co-IP was performed. Total amount of elution loaded was 20 µL after mixing 1:1 with 2X Laemmli sample buffer. The top blot was probed with anti-HA primary antibody for detection of HA tagged prey proteins, using StkP-FLAG^2 as bait. Predicted MWs of proteins are listed in A. The bottom blot was probed with anti-FLAG primary antibody for detection of StkP-FLAG^2. Strains used to prepare extracts were constructed in D39 Δ*cps* strain IU1945. Lane 1, *pbp2x*-HA *stkP*$^+$ (IU6929); lane, 2 *stkP*-FLAG^2 *pbp2x*-HA (IU7510); lane 3, *pbp2b*-HA *stkP*$^+$ (IU6933); and lane 4, *stkP*-FLAG^2 *pbp2b*-HA (IU7512).

Fig. S14. Pairwise co-IP of GpsB-L-FLAG^3 with StkP and MreC, but not with detectable levels of FtsZ, FtsA or PhpP, and pairwise co-IP of StkP-FLAG^2 with MreC, but not with FtsZ, FtsA, or PhpP. Co-IP experiments were performed as described in *Experimental procedures*. A) Western blots of cell lysates before co-IP was performed. Total protein loaded for each sample was 56 µg. The blots shown were probed with native antibodies towards the prey protein of interest or commercial anti-FLAG, as

indicated. Predicted molecular weight (MWs) of FtsZ, FtsA, PhpP, StkP, GpsB-L-FLAG^3, and StkP-FLAG^2 are 44.5, 49.6**,** 27.1**,** 72.3, 16.4, and 74.3 kDa**,** respectively. B) Western blot after co-IP was performed. Total amount of elution loaded was 20 µL after mixing 1:1 with 2X Laemmli sample buffer. Predicted MWs of proteins are listed in A. Strains used to prepare extracts were constructed in D39 Δ*cps* strain IU1945. Lane 1, D39 Δ*cps* (IU1945); lane 2, *gpsB*-L-FLAG^3 (IU5458); and lane 3, *stkP*-FLAG^2 (IU7434).

Fig. S15. Interactions between *Spn* GpsB and other division proteins detected by B2H assays. Hybrid plasmid pairs were co-transformed into the *E. coli* strain BTH101, and interactions were detected by spotting the co-transformation mixtures onto LB-X-gal agar plates, supplemented with the appropriate concentrations of ampicillin and kanamycin and photographed after 40 hours, as described in *Experimental procedures*. A) GpsB-T25, DivIVA-T25, EzrA-T25 and FtsZ-T25 fusions co-expressed with DivIVA-T18, GpsB-T18, EzrA-T18, and FtsZ-T18 fusions, respectively. B) StkP-T25 and StkP-T18 fusions co-expressed with StkP, GpsB, and DivIVA -T18 or -T25, respectively. The bottom panels show the negative (-) and positive (+) controls for the B2H system. White indicates no interactions; blue indicates interactions. See text for additional details.

REFERENCES FOR SUPPLEMENTAL INFORMATION

Ashkenazy, H., S. Abadi, E. Martz, O. Chay, I. Mayrose, T. Pupko & N. Ben-Tal, (2016) ConSurf 2016: an improved methodology to estimate and visualize evolutionary conservation in macromolecules. *Nuc Acids Res* **44**: W344-350.

Evan, G.I., G.K. Lewis, G. Ramsay & J.M. Bishop, (1985) Isolation of monoclonal antibodies specific for human c-myc proto-oncogene product. *Molec Cell Biol* **5**: 3610-3616.

Fadda, D., C. Pischedda, F. Caldara, M.B. Whalen, D. Anderluzzi, E. Domenici & O. Massidda, (2003) Characterization of *divIVA* and other genes located in the chromosomal region downstream of the dcw cluster in *Streptococcus pneumoniae. J Bacteriol* **185**: 6209-6214.

Fadda, D., A. Santona, V. D'Ulisse, P. Ghelardini, M.G. Ennas, M.B. Whalen & O. Massidda, (2007) *Streptococcus pneumoniae* DivIVA: localization and interactions in a MinCD-free context. *J Bacteriol* **189**: 1288-1298.

Holm, L. & P. Rosenstrom, (2010) Dali server: conservation mapping in 3D. *Nuc Acids Res* **38**: W545-549.

Hopp, T.P., K.S. Prickett, V.L. Price, R.T. Libby, C.J. March, D.P. Cerretti, D.L. Urdal & P.J. Conlon, (1988) A short polypeptide marker sequence useful for recombinant protein identification and purification. *Bio-Technol* **6**: 1204-1210.

Hoskins, J., W.E. Alborn, Jr., J. Arnold, L.C. Blaszczak, S. Burgett, B.S. DeHoff, S.T. Estrem, L. Fritz, D.J. Fu, W. Fuller, C. Geringer, R. Gilmour, J.S. Glass, H. Khoja, A.R. Kraft, R.E. Lagace, D.J. LeBlanc, L.N. Lee, E.J. Lefkowitz, J. Lu, P. Matsushima, S.M. McAhren, M. McHenney, K. McLeaster, C.W. Mundy, T.I. Nicas, F.H. Norris, M. O'Gara, R.B. Peery, G.T. Robertson, P. Rockey, P.M. Sun, M.E. Winkler, Y. Yang, M. Young-Bellido, G. Zhao, C.A. Zook, R.H. Baltz, S.R. Jaskunas, P.R. Rosteck, Jr., P.L. Skatrud & J.I. Glass, (2001) Genome of the bacterium *Streptococcus pneumoniae* strain R6. *J Bacteriol* **183**: 5709-5717.

Kelley, L.A., S. Mezulis, C.M. Yates, M.N. Wass & M.J. Sternberg, (2015) The Phyre2 web portal for protein modeling, prediction and analysis. *Nat Protocols* **10**: 845-858.

Land, A.D., H.C. Tsui, O. Kocaoglu, S.A. Vella, S.L. Shaw, S.K. Keen, L.T. Sham, E.E. Carlson & M.E. Winkler, (2013) Requirement of essential Pbp2x and GpsB for septal ring closure in *Streptococcus pneumoniae* D39. *Molec Microbiol* **90**: 939-955.

Lanie, J.A., W.L. Ng, K.M. Kazmierczak, T.M. Andrzejewski, T.M. Davidsen, K.J. Wayne, H. Tettelin, J.I. Glass & M.E. Winkler, (2007) Genome sequence of Avery's virulent serotype 2 strain D39 of *Streptococcus pneumoniae* and comparison with that of unencapsulated laboratory strain R6. *J Bacteriol* **189**: 38-51.

Nováková, L., L. Sasková, P. Pallová, J. Janecek, J. Novotná, A. Ulrych, J. Echenique, M.C. Trombe & P. Branny, (2005) Characterization of a eukaryotic type serine/threonine protein kinase and protein phosphatase of *Streptococcus pneumoniae* and identification of kinase substrates. *FEBS J* **272**: 1243-1254.

Pozzi, G., L. Masala, F. Iannelli, R. Manganelli, L.S. Havarstein, L. Piccoli, D. Simon & D.A. Morrison, (1996) Competence for genetic transformation in encapsulated strains of *Streptococcus pneumoniae*: two allelic variants of the peptide pheromone. *J Bacteriol* **178**: 6087-6090.

Ramos-Montanez, S., H.C. Tsui, K.J. Wayne, J.L. Morris, L.E. Peters, F. Zhang, K.M. Kazmierczak, L.T. Sham & M.E. Winkler, (2008) Polymorphism and regulation of the spxB (pyruvate oxidase) virulence factor gene by a CBS-HotDog domain protein (SpxR) in serotype 2 *Streptococcus pneumoniae. Molec Microbiol* **67**: 729-746.

Rantanen, M.K., L. Lehtio, L. Rajagopal, C.E. Rubens & A. Goldman, (2007) Structure of Streptococcus agalactiae serine/threonine phosphatase. The subdomain conformation is coupled to the binding of a third metal ion. *FEBS J* **274**: 3128-3137.

Schrodinger, L., The PyMOL molecular graphics system, version 1.8.

Tsui, H.C., M.J. Boersma, S.A. Vella, O. Kocaoglu, E. Kuru, J.K. Peceny, E.E. Carlson, M.S. VanNieuwenhze, Y.V. Brun, S.L. Shaw & M.E. Winkler, (2014) Pbp2x localizes separately from Pbp2b and other peptidoglycan synthesis proteins during later stages of cell division of *Streptococcus pneumoniae* D39. *Molec Microbiol* **94**: 21-40.

Tsui, H-C..T., J.J. Zheng, A.N. Magallon, J.D. Ryan, R. Yunck, B.E. Rued, T.G. Bernhardt & M.E. Winkler, (2016) Suppression of a deletion mutation in the gene encoding essential PBP2b reveals a new lytic transglycosylase involved in peripheral peptidoglycan synthesis in *Streptococcus pneumoniae* D39. *Molec Microbiol* **100**: 1039-1065.

Tu, Y., F. Li & C. Wu, (1998) Nck-2, a novel Src homology2/3-containing adaptor protein that interacts with the LIM-only protein PINCH and components of growth factor receptor kinase-signaling pathways. *Mol Biol Cell* **9**: 3367-3382.

Waldo, G.S., B.M. Standish, J. Berendzen & T.C. Terwilliger, (1999) Rapid protein-folding assay using green fluorescent protein. *Nat Biotechnol* **17**: 691-695.

Wayne, K.J., L.T. Sham, H.C. Tsui, A.D. Gutu, S.M. Barendt, S.K. Keen & M.E. Winkler, (2010) Localization and cellular amounts of the WalRKJ (VicRKX) two-component regulatory system proteins in serotype 2 *Streptococcus pneumoniae*. *J Bacteriol* **192**: 4388-4394.

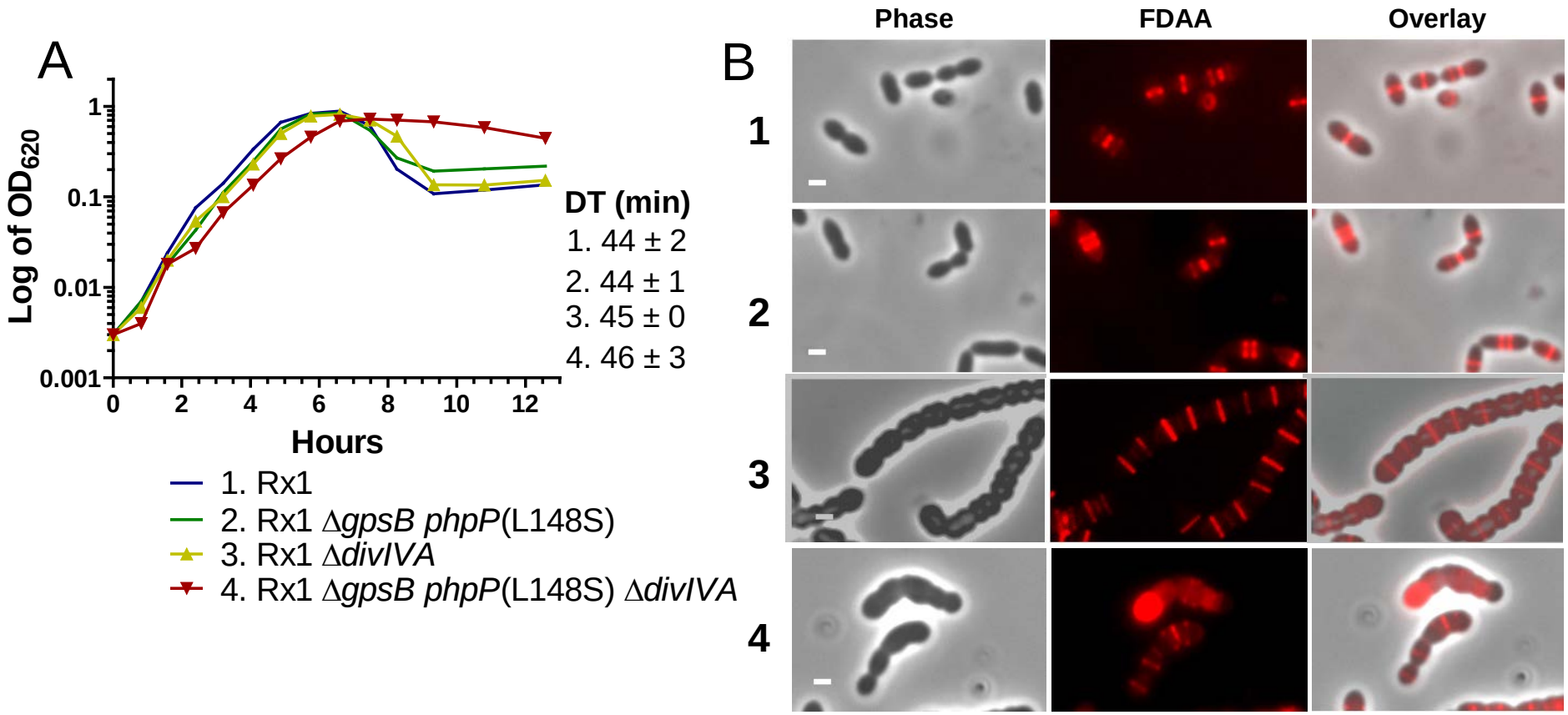
A
Log of OD620
1
0.1
0.01
0.001
0
2
4
6
8
10
12
Hours
DT (min)
1. 44 ± 2
2. 44 ± 1
3. 45 ± 0
4. 46 ± 3
1. Rx1
2. Rx1 ΔgpsB phpP(L148S)
3. Rx1 ΔdivIVA
4. Rx1 ΔgpsB phpP(L148S) ΔdivIVA
B
Phase
FDAA
Overlay
1
2
3
4

Fig. S1

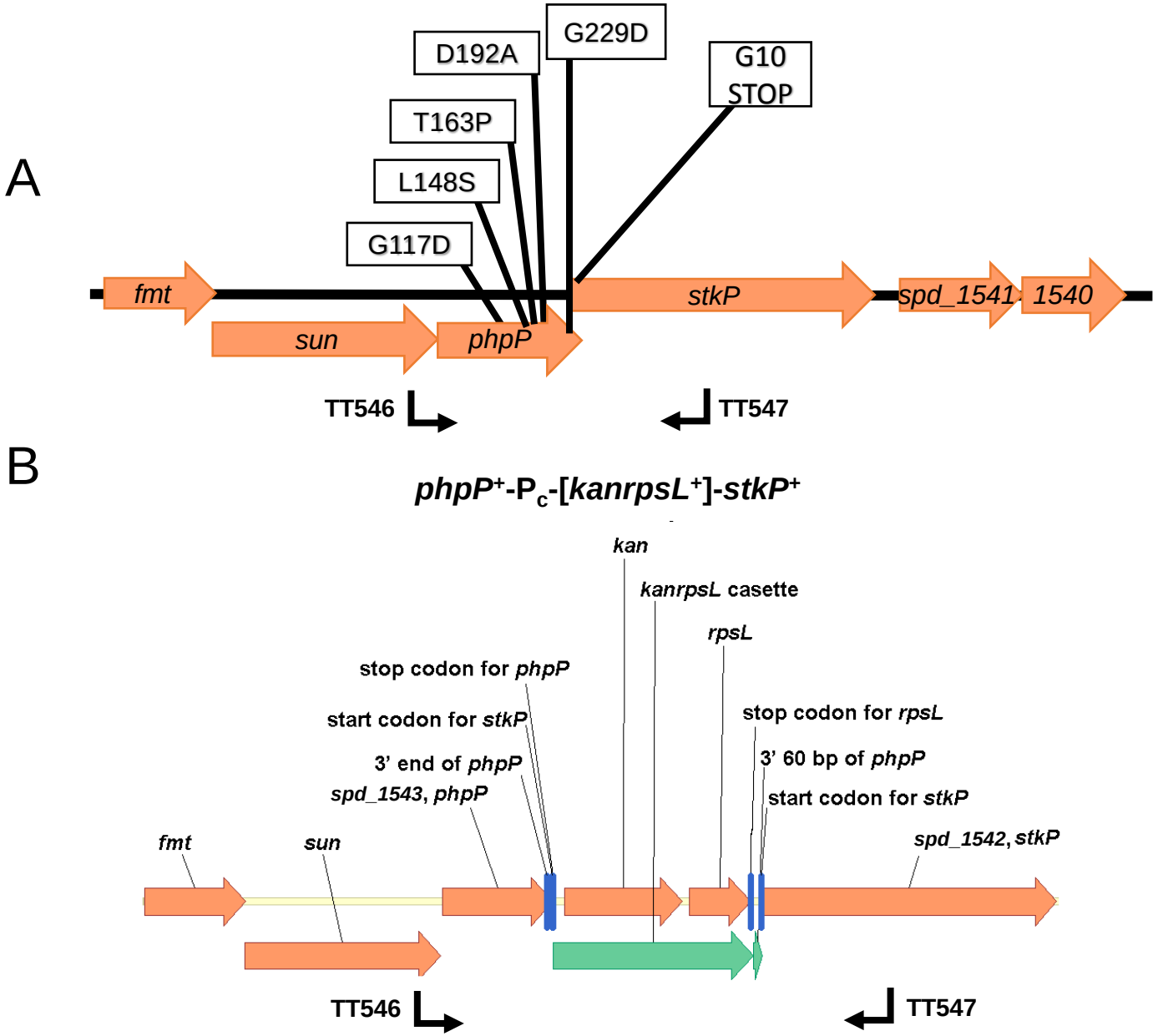
A
D192A
G229D
G10
STOP
T163P
L148S
G117D
fmt
sun
phpP
stkP
spd_1541
1540
TT546
TT547
B
phpP+-Pc-[kanrpsL+]-stkP+
kan
kanrpsL casette
rpsL
stop codon for phpP
start codon for stkP
3' end of phpP
spd_1543, phpP
stop codon for rpsL
3' 60 bp of phpP
start codon for stkP
spd_1542, stkP
fmt
sun
TT546
TT547

Fig. S2

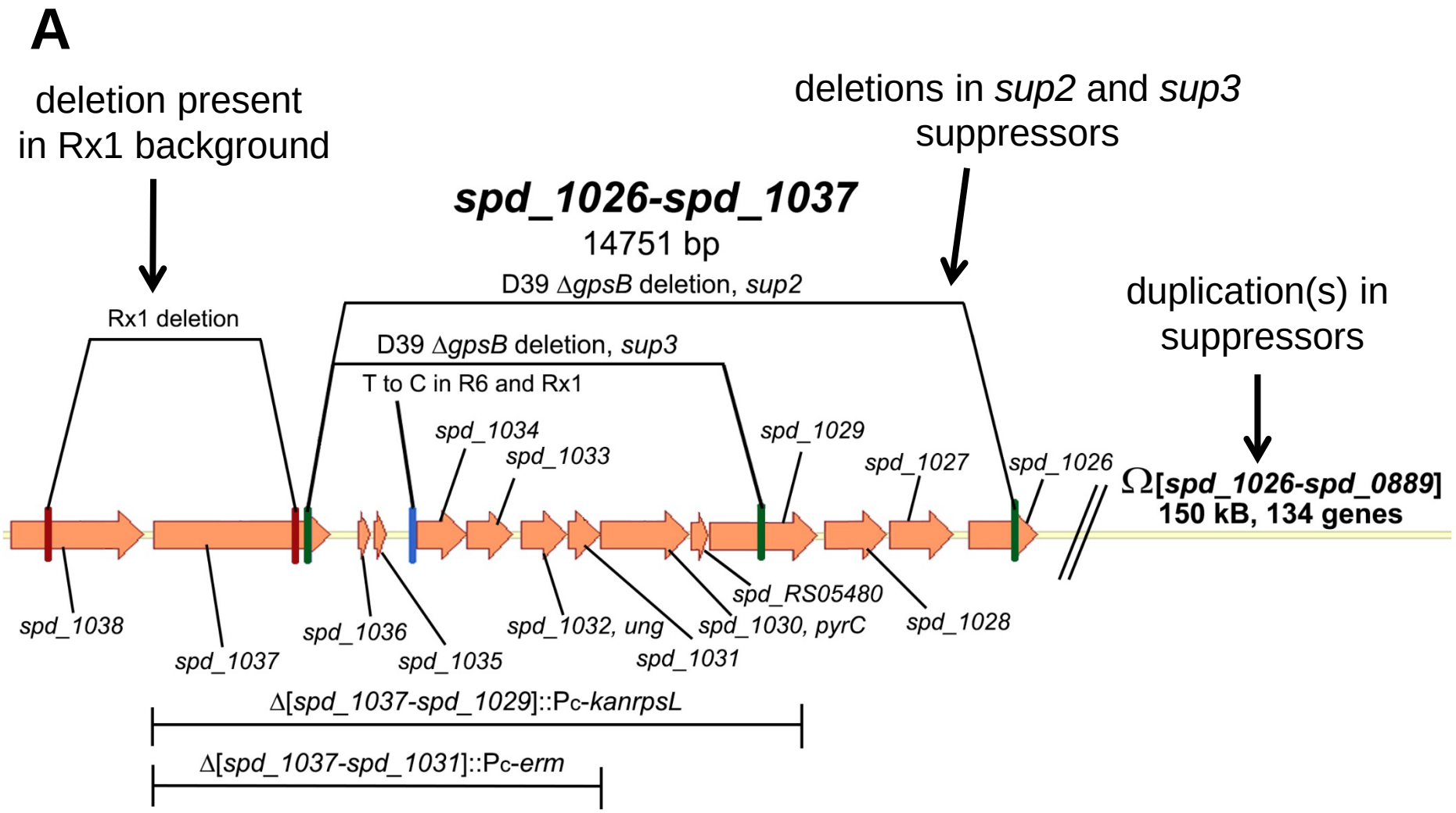
A
deletion present
in Rx1 background
deletions in sup2 and sup3
suppressors
spd_1026-spd_1037
14751 bp
D39 ΔgpsB deletion, sup2
Rx1 deletion
D39 ΔgpsB deletion, sup3
T to C in R6 and Rx1
duplication(s) in
suppressors
spd_1034
spd_1033
spd_1029
spd_1027
spd_1026
Ω[spd_1026-spd_0889]
150 kB, 134 genes
spd_1038
spd_1037
spd_1036
spd_1035
spd_1032, ung
spd_1031
spd_RS05480
spd_1030, pyrC
spd_1028
Δ[spd_1037-spd_1029]::Pc-kanrpsL
Δ[spd_1037-spd_1031]::Pc-erm

Fig. S3A

B

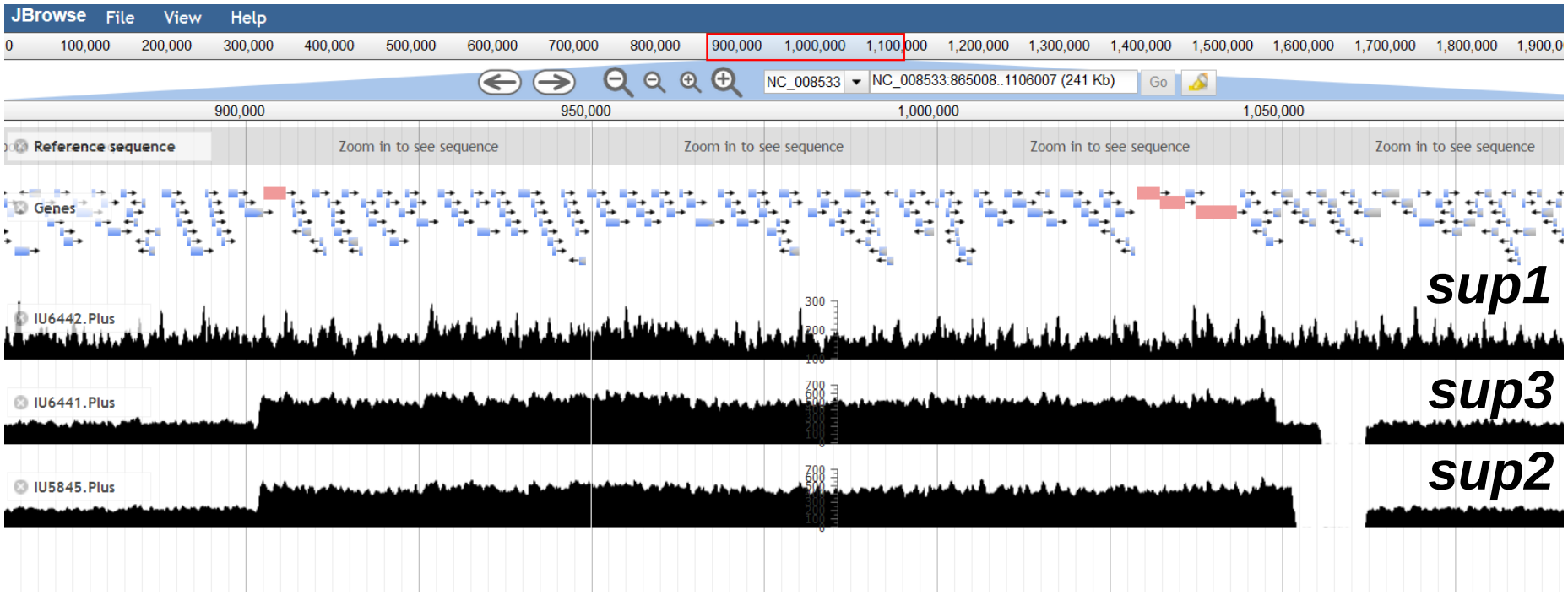
JBrowse
File
View
Help
0
100,000
200,000
300,000
400,000
500,000
600,000
700,000
800,000
900,000
1,000,000
1,100,000
1,200,000
1,300,000
1,400,000
1,500,000
1,600,000
1,700,000
1,800,000
1,900,0
NC_008533
NC_008533:865008..1106007 (241 Kb)
Go
900,000
950,000
1,000,000
1,050,000
Reference sequence
Zoom in to see sequence
Zoom in to see sequence
Zoom in to see sequence
Zoom in to see sequence
Genes
IU6442.Plus
300
200
sup1
IU6441.Plus
700
600
sup3
IU5845.Plus
700
600
sup2

Fig. S3B

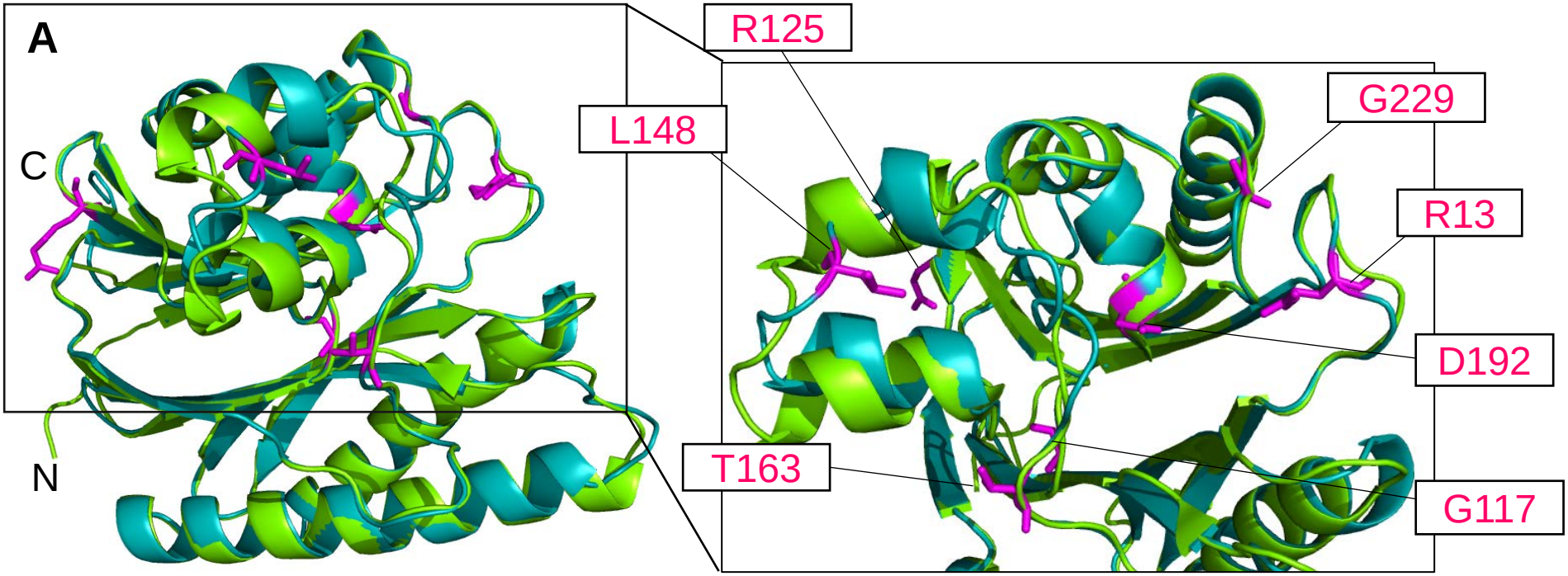
A
C
N
R125
L148
G229
R13
D192
T163
G117

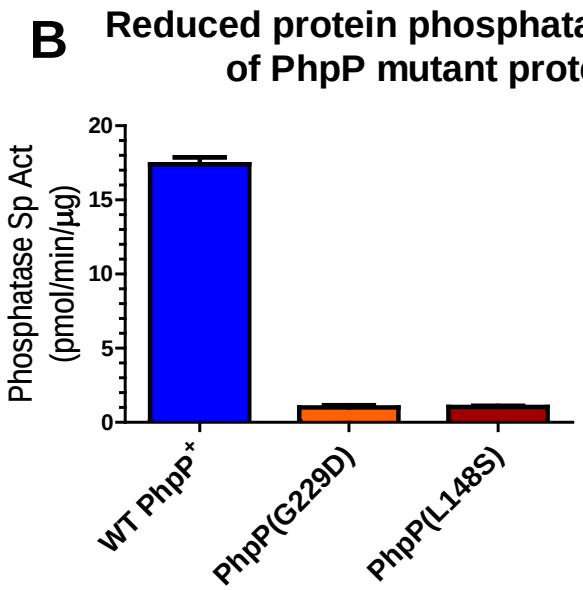
B
Reduced protein phosphatase activity
of PhpP mutant proteins
Phosphatase Sp Act
(pmol/min/µg)
20
15
10
5
0
WT PhpP+
PhpP(G229D)
PhpP(L148S)

Fig. S4

Changes in PhpP suppressors are at conserved amino acids

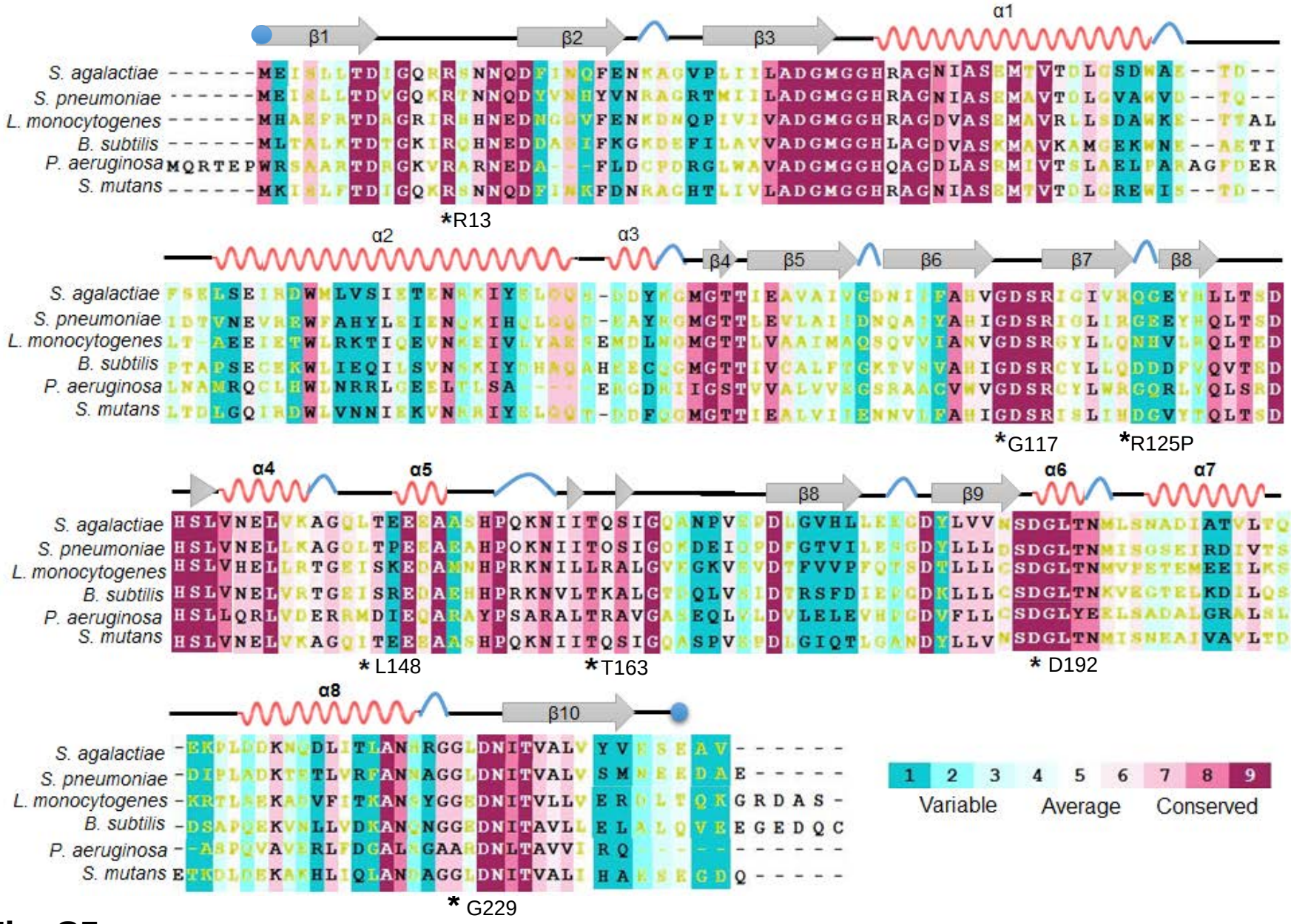

Fig. S5

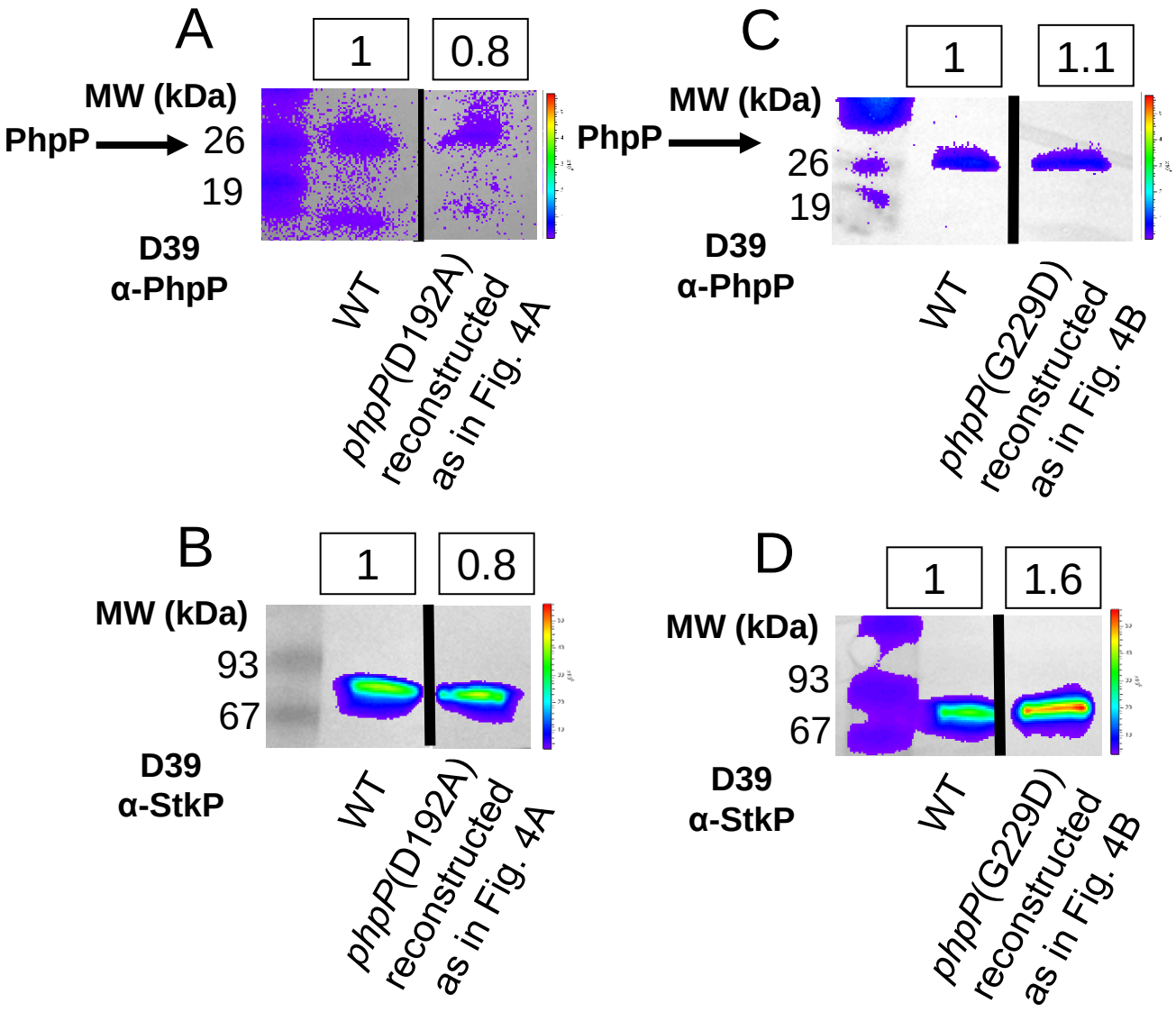
A
1
0.8
MW (kDa)
PhpP
26
19
D39
α-PhpP
WT
phpP(D192A) reconstructed as in Fig. 4A
C
1
1.1
MW (kDa)
PhpP
26
19
D39
α-PhpP
WT
phpP(G229D) reconstructed as in Fig. 4B
B
1
0.8
MW (kDa)
93
67
D39
α-StkP
WT
phpP(D192A) reconstructed as in Fig. 4A
D
1
1.6
MW (kDa)
93
67
D39
α-StkP
WT
phpP(G229D) reconstructed as in Fig. 4B

Fig. S6

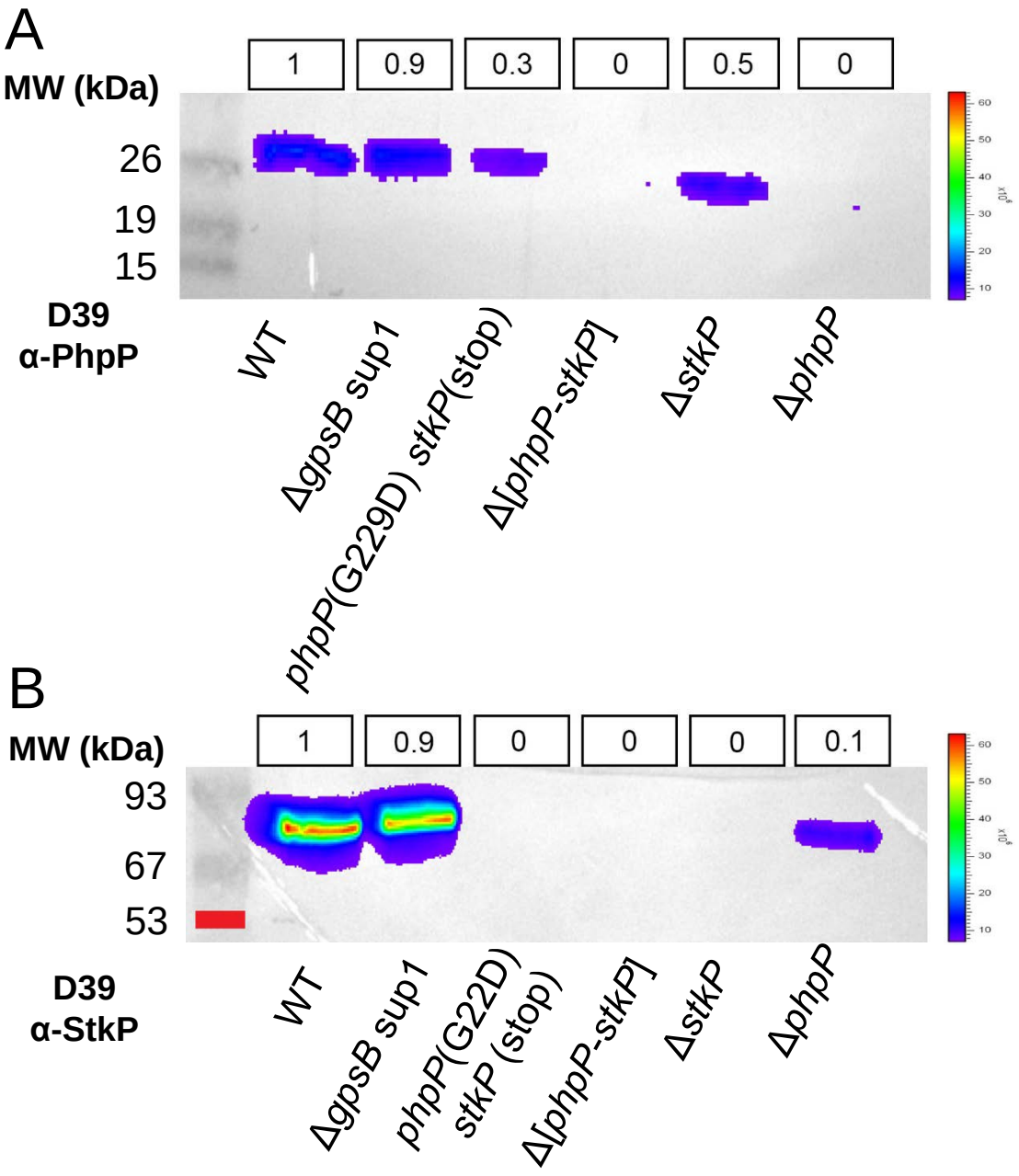
A
MW (kDa)
1
0.9
0.3
0
0.5
0
26
19
15
D39
α-PhpP
WT
ΔgpsB sup1
phpP(G229D) stkP(stop)
Δ[phpP-stkP]
ΔstkP
ΔphpP
B
MW (kDa)
1
0.9
0
0
0
0.1
93
67
53
D39
α-StkP
WT
ΔgpsB sup1
phpP(G22D)
stkP (stop)
Δ[phpP-stkP]
ΔstkP
ΔphpP

Fig. S7

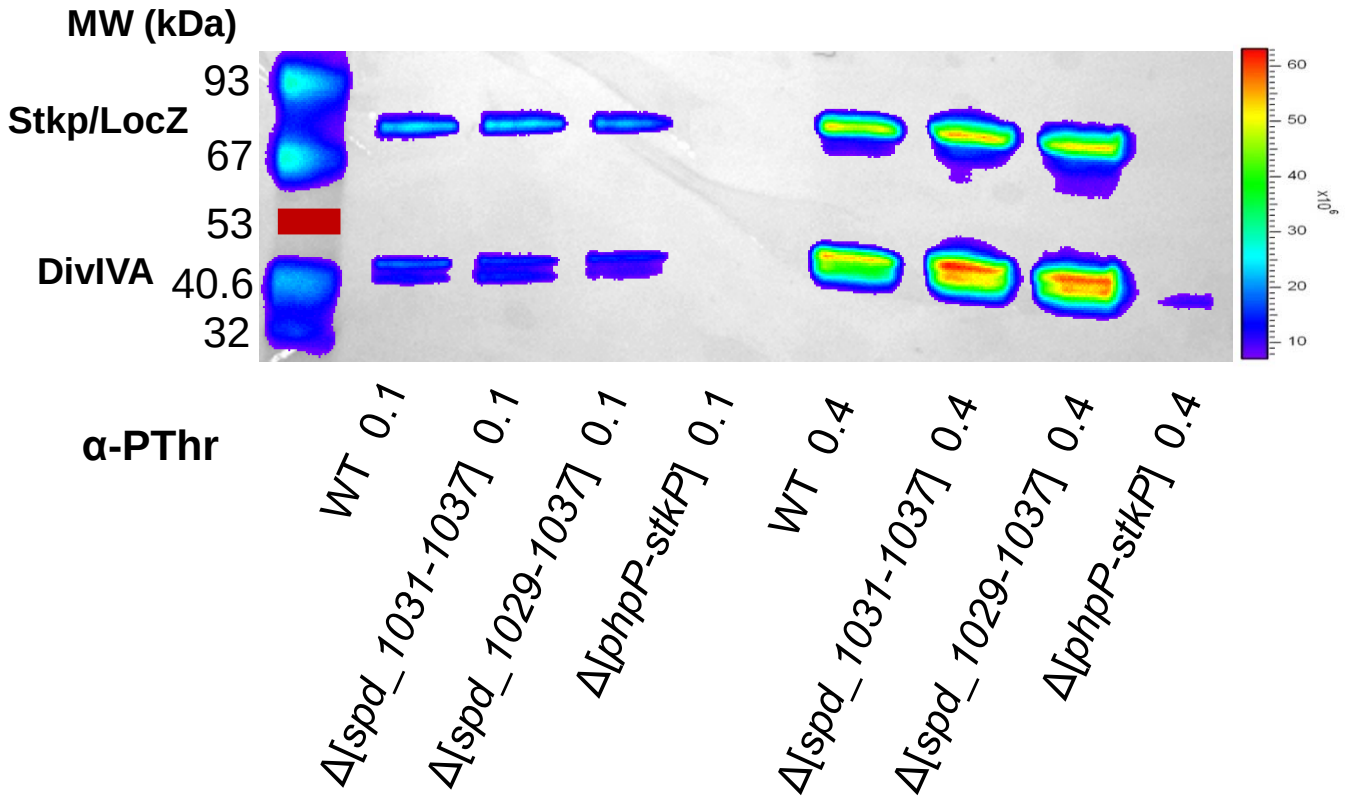
MW (kDa)
93
Stkp/LocZ
67
53
DivIVA
40.6
32
α-PThr
WT 0.1
Δ[spd_1031-1037] 0.1
Δ[spd_1029-1037] 0.1
Δ[phpP-stkP] 0.1
WT 0.4
Δ[spd_1031-1037] 0.4
Δ[spd_1029-1037] 0.4
Δ[phpP-stkP] 0.4
60
50
40
30
20
10
x10⁶

Fig. S8

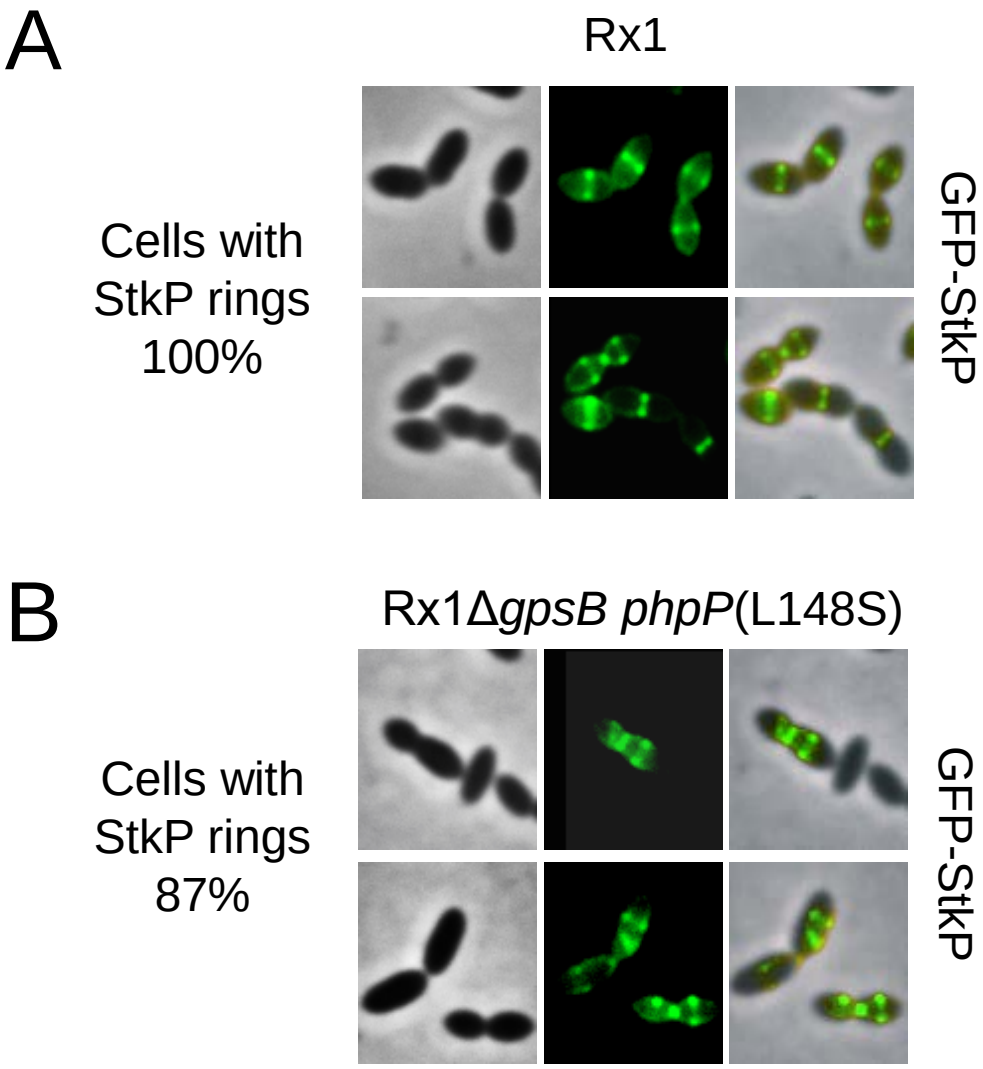
A
Rx1
Cells with StkP rings 100%
GFP-StkP
B
Rx1Δ*gpsB phpP*(L148S)
Cells with StkP rings 87%
GFP-StkP

Fig. S9

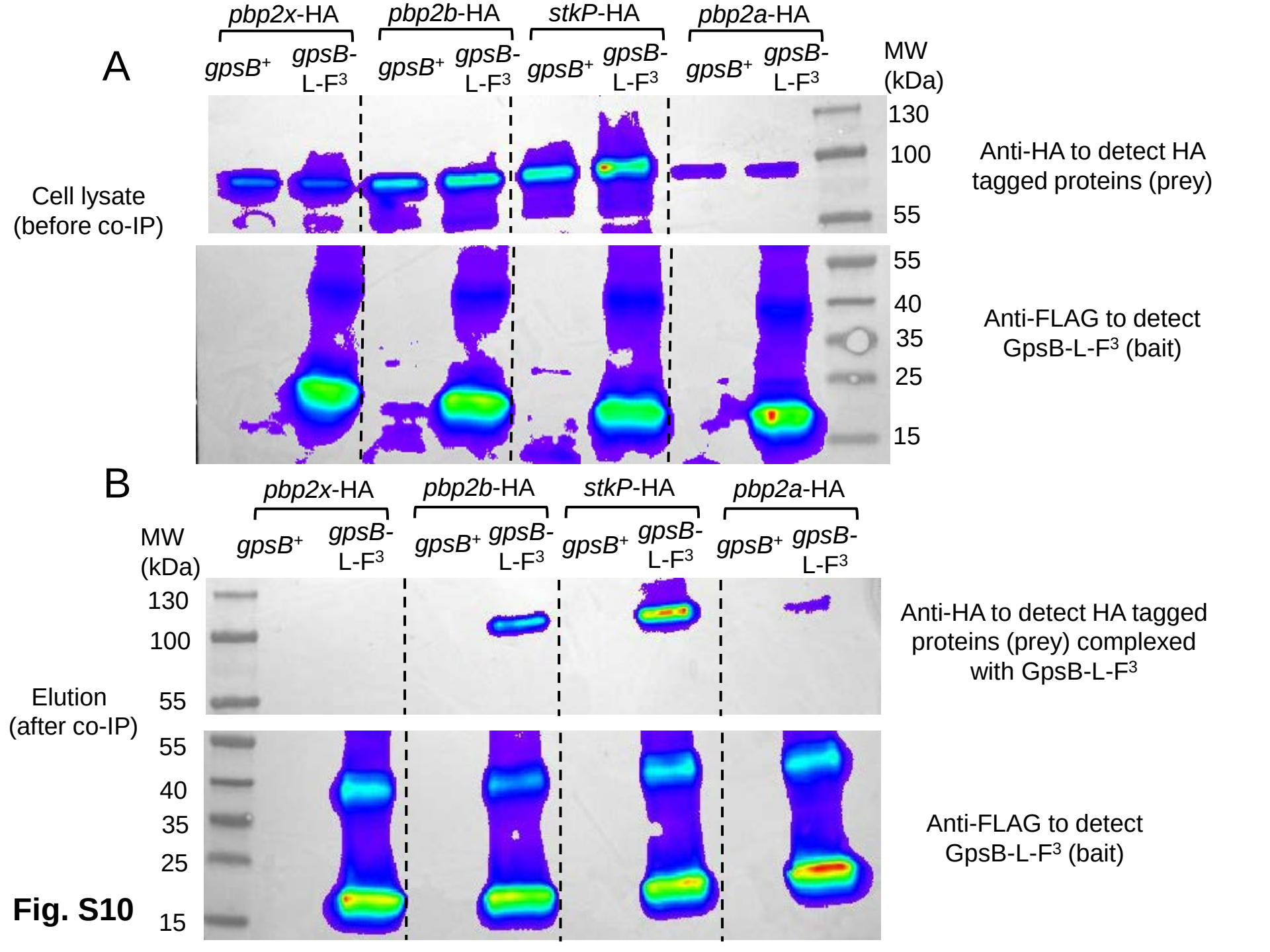
A
pbp2x-HA
pbp2b-HA
stkP-HA
pbp2a-HA
gpsB+
gpsB-L-F3
MW (kDa)
130
100
55
Cell lysate (before co-IP)
Anti-HA to detect HA tagged proteins (prey)
55
40
35
25
15
Anti-FLAG to detect GpsB-L-F3 (bait)
B
Elution (after co-IP)
Anti-HA to detect HA tagged proteins (prey) complexed with GpsB-L-F3
Anti-FLAG to detect GpsB-L-F3 (bait)

Fig. S10

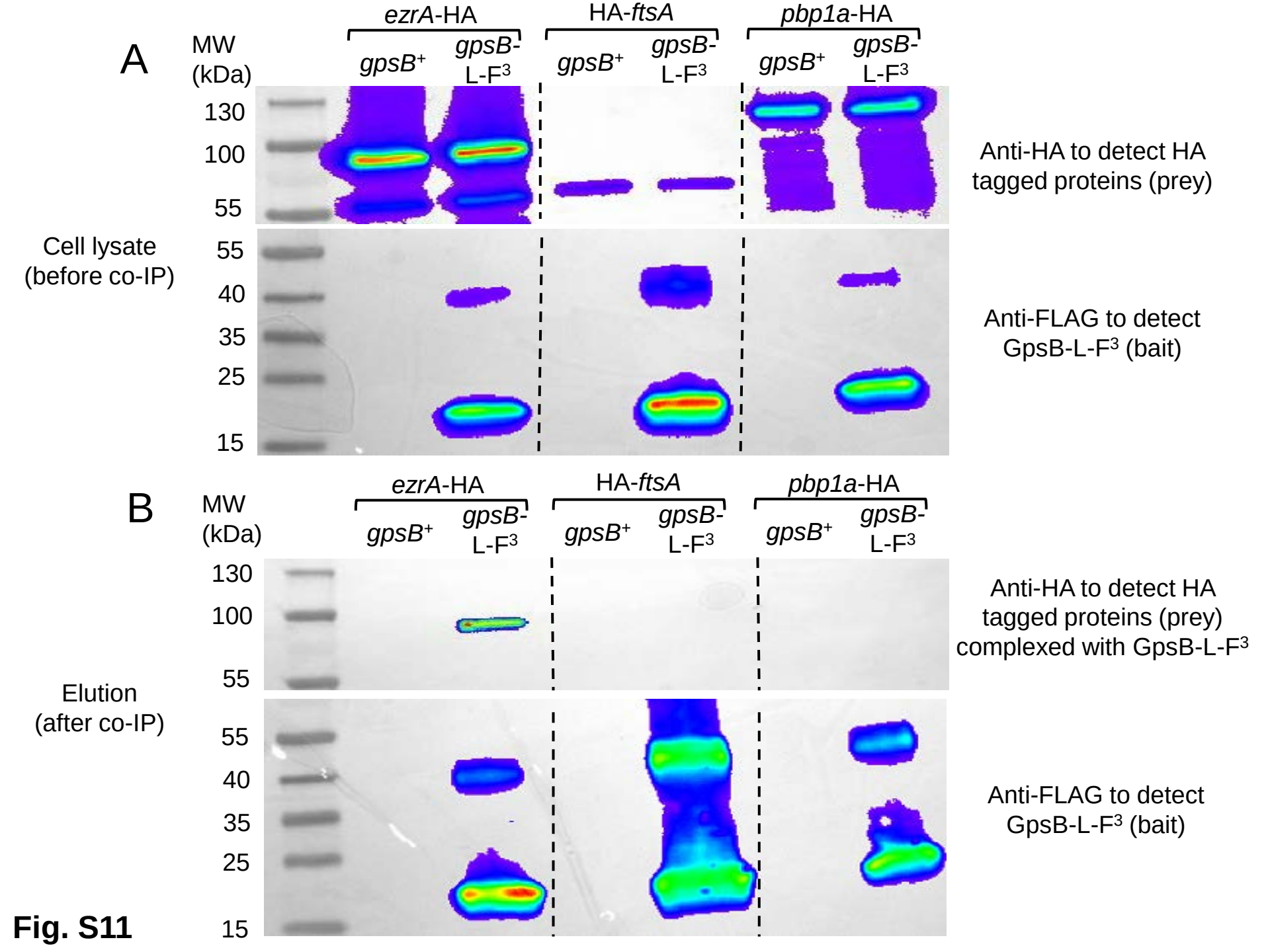
A
MW (kDa)
ezrA-HA
HA-ftsA
pbp1a-HA
gpsB+
gpsB-L-F3
130
100
55
Cell lysate (before co-IP)
55
40
35
25
15
Anti-HA to detect HA tagged proteins (prey)
Anti-FLAG to detect GpsB-L-F3 (bait)
B
MW (kDa)
ezrA-HA
HA-ftsA
pbp1a-HA
gpsB+
gpsB-L-F3
130
100
55
Elution (after co-IP)
55
40
35
25
15
Anti-HA to detect HA tagged proteins (prey) complexed with GpsB-L-F3
Anti-FLAG to detect GpsB-L-F3 (bait)

Fig. S11

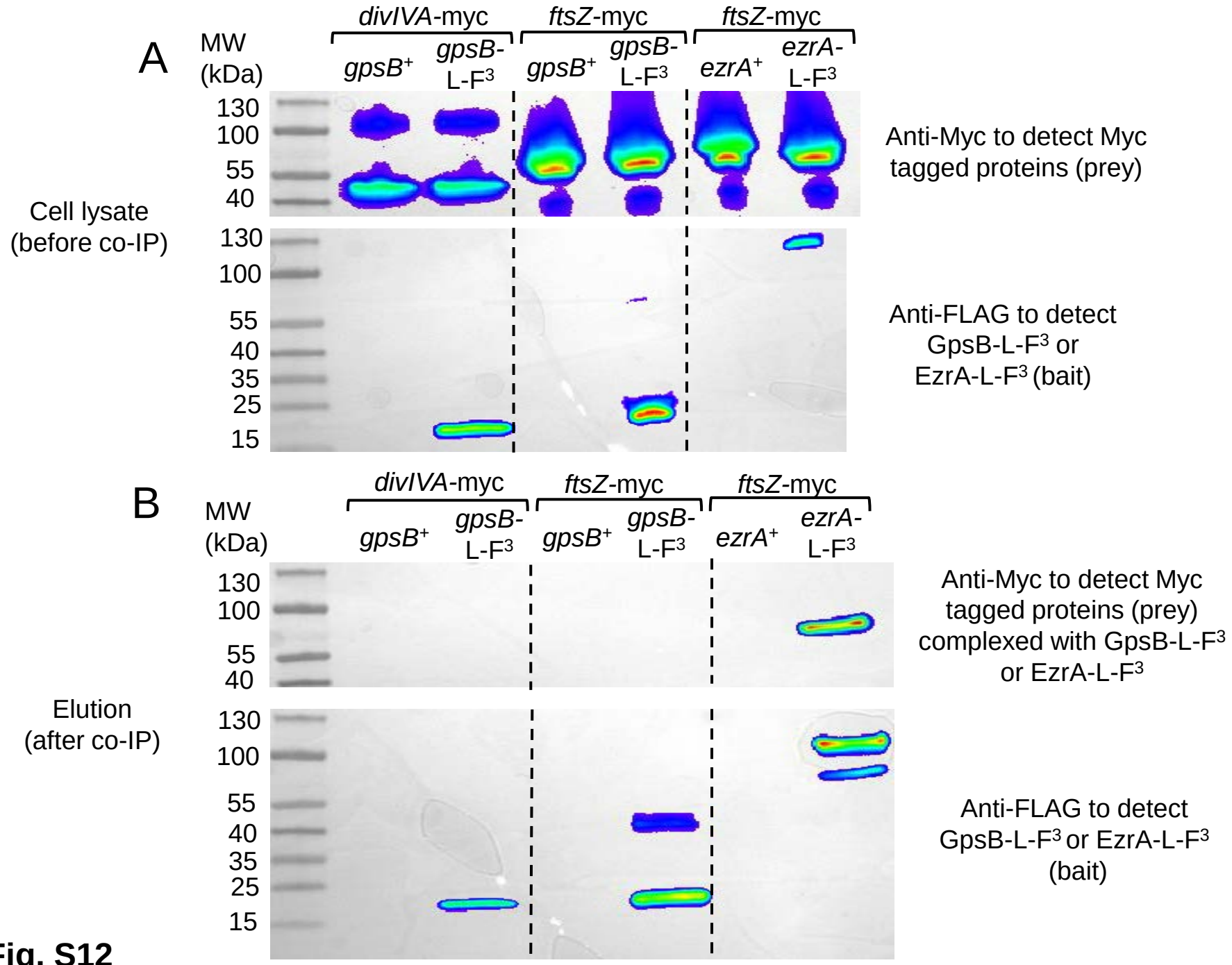
A
MW (kDa)
divIVA-myc
ftsZ-myc
ftsZ-myc
gpsB+
gpsB-L-F3
gpsB+
gpsB-L-F3
ezrA+
ezrA-L-F3
130
100
55
40
Cell lysate (before co-IP)
130
100
55
40
35
25
15
Anti-Myc to detect Myc tagged proteins (prey)
Anti-FLAG to detect GpsB-L-F3 or EzrA-L-F3 (bait)
B
MW (kDa)
divIVA-myc
ftsZ-myc
ftsZ-myc
gpsB+
gpsB-L-F3
gpsB+
gpsB-L-F3
ezrA+
ezrA-L-F3
130
100
55
40
Elution (after co-IP)
130
100
55
40
35
25
15
Anti-Myc to detect Myc tagged proteins (prey) complexed with GpsB-L-F3 or EzrA-L-F3
Anti-FLAG to detect GpsB-L-F3 or EzrA-L-F3 (bait)

Fig. S12

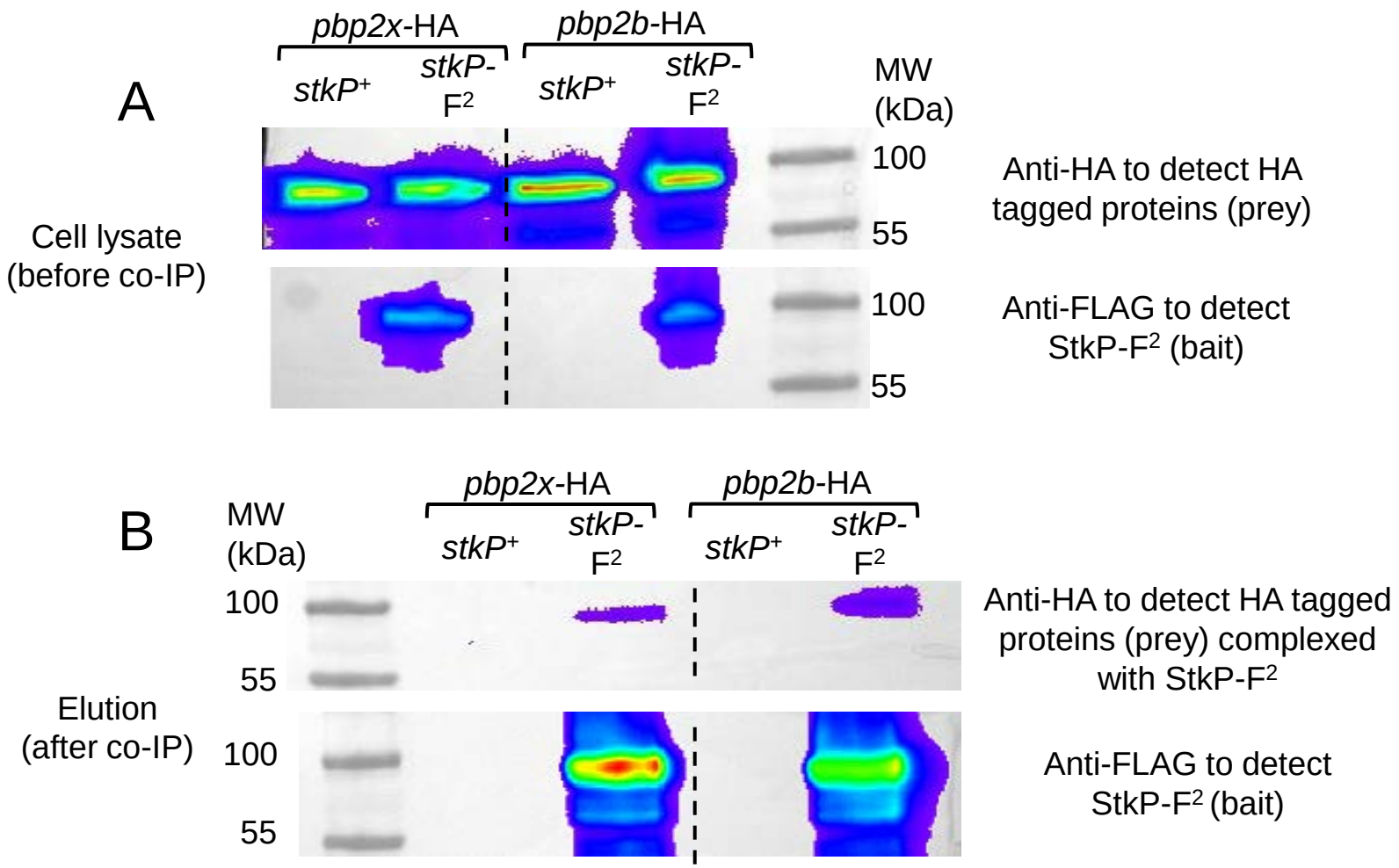
A
pbp2x-HA
pbp2b-HA
stkP+
stkP-F2
stkP+
stkP-F2
MW (kDa)
100
55
Cell lysate (before co-IP)
Anti-HA to detect HA tagged proteins (prey)
100
55
Anti-FLAG to detect StkP-F2 (bait)
B
MW (kDa)
pbp2x-HA
pbp2b-HA
stkP+
stkP-F2
stkP+
stkP-F2
100
55
Elution (after co-IP)
Anti-HA to detect HA tagged proteins (prey) complexed with StkP-F2
100
55
Anti-FLAG to detect StkP-F2 (bait)

Fig. S13

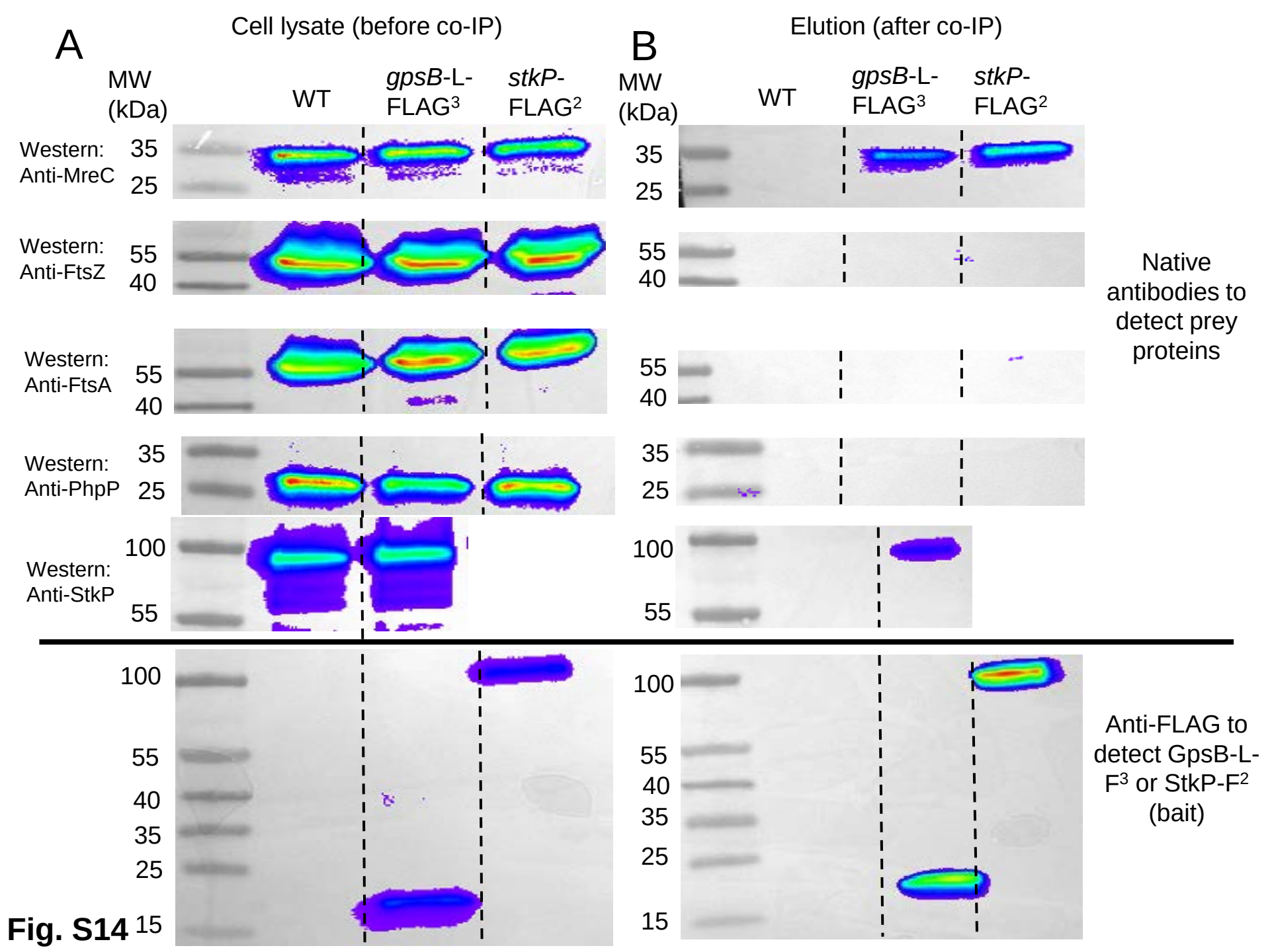
A
Cell lysate (before co-IP)
B
Elution (after co-IP)
MW (kDa)
WT
gpsB-L-FLAG3
stkP-FLAG2
Western: Anti-MreC
Western: Anti-FtsZ
Western: Anti-FtsA
Western: Anti-PhpP
Western: Anti-StkP
35
25
55
40
100
55
Native antibodies to detect prey proteins
100
55
40
35
25
15
Anti-FLAG to detect GpsB-L-F3 or StkP-F2 (bait)

Fig. S14

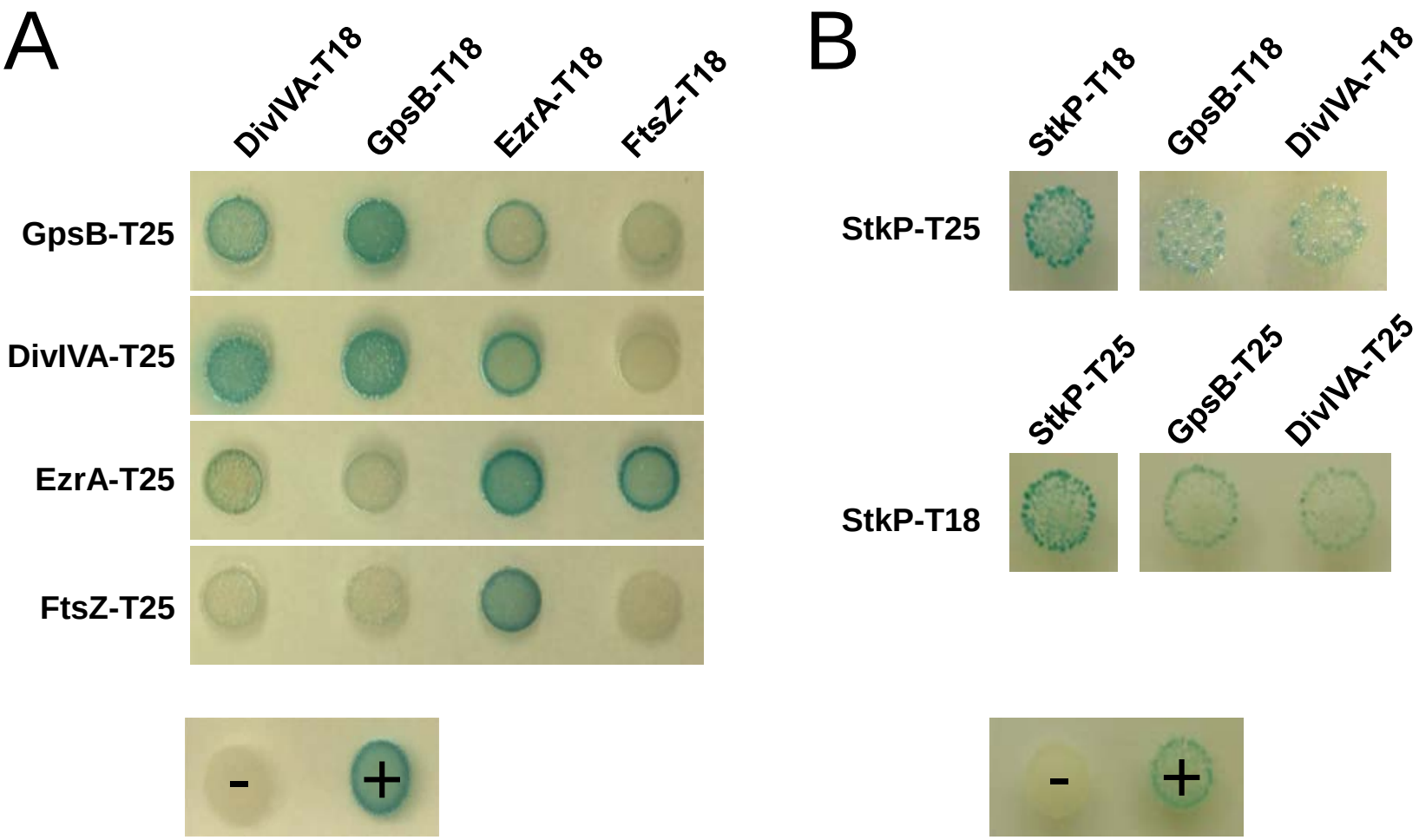
A
DivIVA-T18
GpsB-T18
EzrA-T18
FtsZ-T18
GpsB-T25
DivIVA-T25
EzrA-T25
FtsZ-T25
-
+
B
StkP-T18
GpsB-T18
DivIVA-T18
StkP-T25
StkP-T25
GpsB-T25
DivIVA-T25
StkP-T18
-
+

Fig. S15